WIRELESS ENGINEER

Vol. XXVII FEBRUARY 1950 No. 317

Stresses in Magnetic Fields

THIS is a subject that we considered in the Editorial of December 1946, in which we discussed the lack of agreement on the magnitude of the various stresses. We propose now to draw attention to several points which put the matter beyond any doubt, and entirely remove the vagueness that seemed to envelop the subject.

If a uniformly-wound toroid of wood of cross-section A is split across a diameter, and the two halves pulled apart a short distance δs, the current being adjusted to keep the flux constant, there is no change in H or B in the wood, but there are now the air-gaps of total volume $2A.\delta s$ with their magnetic energy of $H^2/(8\pi)$ ergs per cubic cm. As this energy must be equal to the work done in pulling the two halves apart, the force exerted must be $2AH^2/(8\pi)$, that is $H^2/(8\pi)$ dynes per cm^2; we use c.g.s.e.m. units in which B and H in air are numerically equal. The same would be true without the wooden ring, which is merely a support for the winding.

How and where is this pull exerted by the field? On the turns of wire which carry current in the magnetic field due to all the other turns. Every part of a turn experiences a force tending to increase the size of the turn, but as the magnetic field is stronger on the inside of the ring because of the shorter path, there is a resultant force tending to move the turn towards the centre of the ring.

If we now introduce an iron ring instead of the wooden one, with the same initial current as before, there will be no change in H in the material of the ring, and no change in the magnetic field in which the winding is situated, and consequently no change in the forces on the winding, or the resultant catapult action of the winding in opposing the applied pull. This must still be equal to $H^2/(8\pi)$ dynes per cm^2 of cross-section. But from the energy now stored in the air-gap we find that the total pull must equal $B^2/(8\pi)$ dynes per cm^2; hence the forces on the iron must account for the difference $B^2(1-1/\mu^2)/(8\pi)$ or $BH(\mu-1/\mu)/(8\pi)$. As before, we assume that, as the small air-gap is made, the current is increased so as to keep the flux, and therefore B and H in the iron constant. The field in which the winding is situated will also be unchanged. In the gap $H_g = B$.

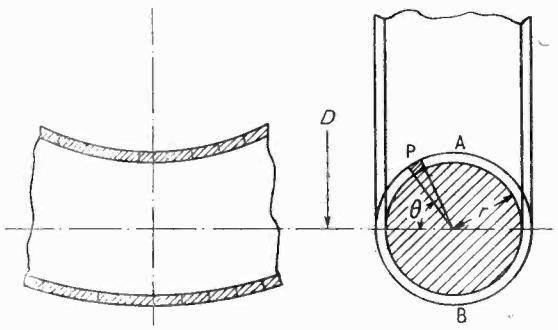

Fig. 1

Returning to the wooden ring, we will now calculate the forces on the winding in the ordinary way, in order to confirm that it gives the same result as that obtained from the energy in the air-gap.

Fig. 1 shows a section of a part of the ring uniformly wound with rectangular strip, which for simplicity of calculation is assumed to be in close contact. The value of H falls to zero over the thickness of the strip, so that the mean

value will be half that at the inner surface. At A the length of the magnetic path is $\pi(D - 2r)$ whereas at B it is $\pi(D + 2r)$. At P the mean value of H will be

$$\frac{\text{m.m.f.}}{2\pi(D - 2r\sin\theta)}$$

and the radial force on the piece of wire $rd\theta$ at P carrying a current I will be

$$\frac{I}{10} \times \frac{\text{m.m.f.}}{2\pi(D - 2r\sin\theta)} \times rd\theta.$$

Its component parallel to AB will be this multiplied by $\sin\theta$, and on integrating this over the whole turn, we have

$$\frac{I}{10} \times \frac{\text{m.m.f.} \times r}{2\pi D} \int^{2\pi} \frac{\sin\theta\, d\theta}{1 - \frac{2r}{D}\sin\theta}$$

$$= \frac{Ir}{20\pi D} \times \text{m m.f.} \times \frac{2\pi r}{D} \text{ approximately,}$$

since $2r/D$ is assumed to be small.

The number of turns per cm of mean periphery is $T/(\pi D)$, and the resultant inward force per cm of periphery will be

$$\frac{IT}{\pi D} \times \frac{r}{20\pi D} \times \frac{4\pi IT}{10} \times \frac{2\pi r}{D} = \frac{4}{100} \cdot \frac{I^2T^2r^2}{D^3}.$$

The total upward force on the lower half of the ring will be D times this, that is,

$$\frac{4}{100} \cdot \frac{I^2T^2r^2}{D^2} \text{ and putting } H = \frac{4\pi}{10} \cdot \frac{IT}{\pi D}$$

this becomes

$$H^2r^2/4 \text{ dynes.}$$

Dividing this by $2A(=2\pi r^2)$ we get $H^2/(8\pi)$ dynes for the force per cm² of cross-section.

The same result can be obtained more simply by assuming the toroid to have a square cross-section. In the integration we made an approximation, but it should be noted that the value of B in the air-gap varies from point to point, and the usual formula $B^2/(8\pi)$ is an approximation to the mean square. By assuming a uniformly-wound toroid the nature of the field is accurately prescribed and one is not troubled with magnetic leakage.

Divergent Views

In the December 1946 Editorial we pictured the lines of force crossing each square cm of the gap, splitting up into two components H and $4\pi J$, the former of which passes through the surface into the iron while the latter ends on the surface polarity. In all these formulae H is the magnetic force in the iron and not in the gap. The polarity or intensity J per unit area is equal to $(B - H)/(4\pi)$.

It is in calculating the mechanical force on J that the uncertainty arises. Is the effective field strength to be employed equal to $2\pi J$ or to $H + 2\pi J$; that is, does the H that passes through the surface into the iron play any part in exerting force on the surface polarity? If not, then the force per cm² on the polar surface is equal to

$$\frac{B - H}{4\pi} \times \frac{B - H}{2} = \frac{B^2}{8\pi} - \frac{BH}{4\pi} + \frac{H^2}{8\pi}$$

$$= \frac{B^2}{8\pi}\left(1 - \frac{2}{\mu} + \frac{1}{\mu^2}\right)$$

which was the result arrived at by Maxwell. Since the total tension per cm² is $B^2/(8\pi)$, the difference must be the tension in the field which has passed into the iron, and this must be equal to

$$\frac{B^2}{8\pi}\left(\frac{2}{\mu} - \frac{1}{\mu^2}\right)$$

We have now seen that a part of this [viz., $H^2/(8\pi)$] represents the force on the windings. This leaves

$$\frac{B^2}{8\pi}\left(\frac{2}{\mu} - \frac{2}{\mu^2}\right) = \frac{BH}{4\pi}\left(1 - \frac{1}{\mu}\right)$$

for the part of the air-gap force per cm² which acts throughout the iron with a sort of catapult action.

The total force is made up of three components, the direct pull on the pole-face, the tension of the field which is converted into lateral forces acting on the iron, and the tension of the field which is converted into lateral forces on the windings. Generally speaking, only the first is of any practical importance. Maxwell's view that the forces in the iron may be regarded as made up of a uniform pressure of $H^2/(8\pi)$ in every direction (not only transverse to the field) and a tension of $BH/(4\pi)$ in the direction of the field, gives a resultant tension along the field equal to the difference, that is,

$$\frac{B^2}{8\pi}\left(\frac{2}{\mu} - \frac{1}{\mu^2}\right)$$

which agrees with the result obtained above.

In the 1946 Editorial we referred to the fact that Helmholtz disagreed with Maxwell, and that a different result was obtained by Moullin by assuming that the effective field strength acting on the polarity of the pole-face is not $2\pi J$ but $H + 2\pi J$. This seems more probable, for it is difficult to see why the field H should not exert any force on the surface polarity. On this assumption the force on 1 cm² would be

$$J(H + 2\pi J) = \frac{B - H}{4\pi}\left(H + \frac{B - H}{2}\right)$$

$$= \frac{B^2 - H^2}{8\pi} = \frac{B^2}{8\pi}\left(1 - \frac{1}{\mu^2}\right)$$

Since the total force is $B^2/(8\pi)$ and the force

to be transmitted to the winding is $H^2/(8\pi)$, this is undoubtedly the total force acting on the iron. Hence the assumption made by Moullin gives the total lifting force exerted on the iron, as distinct from that on the winding, and it naturally vanishes when $\mu = 1$. If this assumption were correct, the total force would only be divided into two components, that on the pole-face and that transmitted through the iron to the winding. We show later that neither Maxwell nor Moullin make the correct assumption.

We shall now consider an iron ring of square cross-section uniformly wound: if the side of the square is s and the inner, outer and mean diameters are D_i, D_o, and D respectively, and H_i, H_o and H the corresponding values of the magnetic force, then assuming with Maxwell that there is a lateral pressure of $H^2/(8\pi)$, the pressure at the inner surface on an element subtending an angle $d\theta$, and therefore having an area of $(D_i/2)d\theta \times s$, will be

$$\frac{H_i^2}{8\pi} \times \frac{D_i}{2} \cdot s \cdot d\theta$$

The pressure at the outer surface will be

$$\frac{H_o^2}{8\pi} \times \frac{D_o}{2} \cdot s \cdot d\theta$$

The resultant force on the element will act towards the centre of the ring and will be equal to the difference

$$(H_i^2 D_i - H_o^2 D_o) \frac{s}{16\pi} \cdot d\theta$$

For the total radial force on the half ring we put $\int d\theta = \pi$, and for the resultant upward component we must multiply by $2/\pi$; this gives for the total upward force

$$(H_i^2 D_i - H_o^2 D_o) \frac{s}{8\pi}$$

which, since $H_i D_i = H_o D_o = HD$,

$$\frac{H_i}{H} = \frac{D+s}{D} = 1 + \frac{s}{D} \text{ and}$$

$$\frac{H_o}{H} = \frac{D-s}{D} = 1 - \frac{s}{D}$$

is equal to $H^2 D \left[\left(1 + \frac{s}{D}\right) - \left(1 - \frac{s}{D}\right) \right] \frac{s}{8\pi}$

that is $\frac{H^2 \cdot 2s^2}{8\pi}$.

Since the area of the two gaps is $2s^2$, this corresponds to a force of $H^2/(8\pi)$ per cm² of gap area.

This is a very interesting result, which might have been foreseen. If the lateral pressure in the field, whether in air or iron, is equal to $H^2/(8\pi)$, then there is no change in this pressure on passing from the iron into the air at the surface, but as one passes through the winding, H falls to zero and with it the lateral pressure which is taken up by the winding. Hence, on this assumption, the lateral pressure in the iron is transmitted to the winding and there is no separate radial force on the iron itself.

This agrees with the assumption that there is a tension of $H^2/(8\pi)$ along the lines of force and a lateral pressure of $H^2/(8\pi)$, but it does not agree with Maxwell's assumption that the tension along the lines is equal to $BH/(4\pi) - H^2/(8\pi)$. It is difficult to see how Maxwell's assumption can explain the facts. If a rubber band were passed half round a cylinder and stretched as shown in Fig 2 it would exert radial forces on the cylinder, and the resultant of all the radial forces acting on the cylinder must be equal to the sum of the tensions on the two sides. In the magnetic case we find that the resultant of all the radial forces is equivalent to $H^2/(8\pi)$ that is $B^2/(8\pi\mu^2)$ on each square centimetre of the air-gaps and this must surely be equal to the tension in the field. If this is so, then the total force per cm² in the gap $B^2/(8\pi)$ is simply divided into two components, one $B^2(1 - 1/\mu^2)/8\pi$ exerting its force on the pole-face—the force then being transmitted mechanically throughout the iron—and the other $B^2/(8\pi\mu^2)$ which is transmitted magnetically through the iron to exert by catapult action a lateral pressure which is exerted on the windings. This agrees with the result obtained on Moullin's assumption.

Fig. 2 indicates clearly what we mean by the term 'catapult action.'

Fig. 2.

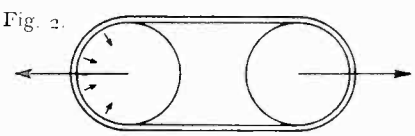

The Correct Solution

Having thus explained the divergent views and the resulting confusion, we shall now show that the matter can be settled quite simply and definitely.

If the air-cored toroid be immersed in a medium of permeability μ, the flux density B and the forces on the conductor, with the same current as before, will be increased to μ times their previous values. Hence the tension in the field and the lateral pressure will also be increased in the same ratio; both will now be $HB/(8\pi)$ or $\mu H^2/8\pi$ per cm².

This is easily confirmed by considering the force between two parallel conductors in a medium of permeability μ. If the two conductors carry equal currents I in opposite directions, as in Fig. 3 (a), the force on each conductor per cm of length due to the field of the other is

$I^2\mu/(100a)$. The value of H at the point P is $4Ia/(10r^2) = 4I\cos^2\theta/(10a)$ and on integrating $\mu H^2/(8\pi)$ over the whole mid-plane, that is from $\theta = -\pi/2$ to $\theta = +\pi/2$ one obtains $I^2\mu/(100a)$ per cm of length of conductor, which agrees with the repulsive force between the conductors.

Similarly, if the currents are in the same direction, as in Fig 3 (b) the value of H at the point P is $4Ib/(10r^2) = 4I \sin\theta \cos\theta/(10a)$, which, on integrating $\mu H^2/8\pi$ from $\theta = -\pi/2$ to $\theta = +\pi/2$ gives $I^2\mu/(100a)$, which again agrees with the force, in this case attractive, between the two conductors. There is, therefore, no doubt whatever that in a medium of permeability μ the longitudinal tension and the lateral pressure are both equal to $\mu H^2/(8\pi)$ or $BH/(8\pi)$ or $B^2/(8\pi\mu)$.

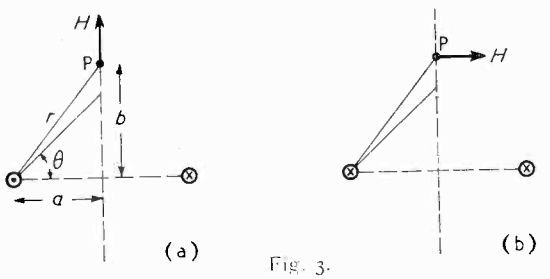

Fig. 3.

As the total force per cm² in the air-gap of the electromagnet is $B^2/(8\pi)$ and the magnetic tension in the iron is $BH/(8\pi)$, the force acting on the pole-face must be the difference, viz.

$$\frac{B^2}{8\pi} - \frac{BH}{8\pi} = \frac{B}{8\pi}(B - H) = \frac{B}{8\pi} \times 4\pi J = \frac{B}{2} \times J$$

Hence the correct result is obtained by multiplying the intensity of magnetization J, not by $(B - H)/2 = 2\pi J$, as Maxwell assumed, nor by $(B + H)/2 = H + 2\pi J$, as Moullin assumed, but by $B/2$.

Turning again to the iron ring of square section with its uniform winding, we can see now that the radial pressure per cm² drops from $BH/(8\pi)$ to $H^2/(8\pi)$ on passing through the surface from the iron into the air, and then from $H^2/(8\pi)$ to zero on passing through the winding.

Of the total force $B^2/(8\pi)$ per cm² in the air-gap, the greater part [viz., $(1 - 1/\mu)B^2/(8\pi)$] acts on the pole-face; the remainder $B^2/(8\pi\mu)$ passes into the iron as a magnetic tension, and causes two catapult forces, one on the iron itself, equal to $(1/\mu - 1/\mu^2)B^2/(8\pi)$, and the other on the winding, equal to $B^2/(8\pi\mu^2)$ per cm².

Much of this is only of academic interest, as $1/\mu^2$ is generally negligible compared with unity, and the magnetic circuit is rarely wound uniformly. If, in the above examples, the winding were limited to the upper half of the ring, even if the total ampere-turns were the same, magnetic leakage would cause the flux in the ring to vary from point to point around the ring.

If the air-gap is negligibly small, the total pull, and the part of it that acts on the pole-face, can be calculated from the flux crossing the gap. If the gap is not negligible, fringing will have to be taken into account. Although there may be no winding on the lower half, the tangential H is the same just outside the ring as it is just inside, and, on passing from iron to air, the lateral stress will fall from $BH/(8\pi)$ to $H^2/(8\pi)$, but as there is no current-carrying winding to take up the latter stress, it will be taken up by the leakage field. We do not propose, however, to go more fully into this aspect of the problem.

G. W. O. H.

ALIGNED-GRID VALVES

Distribution of Current Density

By D. C. Rogers, A.M.I.E.E.

(Standard Telephones and Cables, Ltd.)

SUMMARY.—The electron beam from the cathode of an amplifier valve is focused into well-defined beams by the action of the electric field in the region of the control grid. In aligned-grid valves, use is made of this phenomenon by placing the screen-grid wires in positions where they will intercept only a small fraction of the total cathode current.

Owing to the doubtful validity of the existing theoretical treatment of the subject, an experimental study of the current-density distribution in these electron beams was undertaken for the purpose of determining the best position of the screen wires.

It is often assumed that the grid-to-screen distance should be such that the focus of the electron beam lies in the plane of the screen. The measurements described here show that this is not necessarily true and that a lower screen current will usually be obtained with a smaller grid-to-screen distance.

LIST OF SYMBOLS

a = Grid pitch, measured between centres of grid wires.
d = Grid-wire diameter.
l_g = Cathode-grid distance.
l_a = Cathode-anode distance in a triode, or cathode-screen distance in a tetrode.
l_a-l_g = Grid-anode distance in a triode, or grid-screen distance in a tetrode.
V_g = Grid potential with respect to cathode (e.s.u.)
V_a = Anode potential of a triode or screen voltage of a tetrode with respect to cathode. (e.s.u.)
V_o = Potential in the grid plane. (e.s.u.)
e = Electron charge (e.s.u.)
m = Electron mass.
I = Current flowing between two grid wires, per unit length of grid wire. (e.s.u.)
J = Cathode-current density (e.s.u.)
y = Distance co-ordinate measured parallel to the cathode surface and perpendicular to the grid wires.
z = Distance co-ordinate measured perpendicular to the cathode surface.
V_d = The anode potential of an equivalent diode (e.s.u.) (See Appendix I.)
s = The cathode-anode distance of an equivalent diode. (See Appendix I).
v = Electron velocity (cm/sec)
t = Time in seconds.
$\mathcal{E}$ = Electrostatic field (e.s.u.)
μ = Amplification factor.

1. Introduction

In pentode or beam tetrode valves, it is often found that the power-handling capacity is limited by the maximum permissible screen-grid dissipation and, accordingly, much attention has been devoted to the positioning of the screen wires in the shadow of those of the control grid, in order to intercept a minimum fraction of the cathode current. In receiving-type amplifying valves, too, the reduction of screen current is of considerable importance since the noise current generated by such valves is largely dependent on the amount of current falling on the screen.

MS accepted by the Editor, June 1949

It has long been known that in the useful operating range of most valves the electrostatic field in the region of the control-grid causes the electrons to be deflected towards a plane midway between the grid wires. Some typical electron paths in the cathode-grid and grid-screen regions are shown in Fig. 1. Bull[1] has shown that the apertures between the grid wires form cylindrical electron lenses and has shown how their focal lengths can be determined, using the method of Davisson and Calbick[2,3].

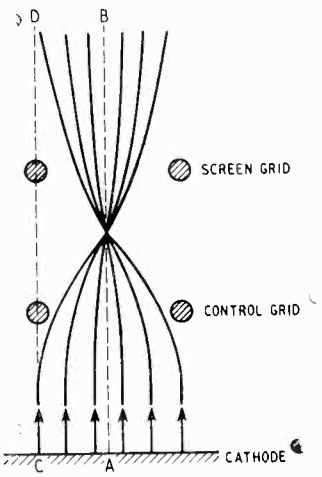

Fig. 1. *Typical electron paths in an aligned-grid valve.*

In practice it is found that the screen current is not reduced to zero, as would be expected if the electron beams came to perfect foci; this fact could be attributed to one or more of the following causes:

(a) The lenses formed by the grid apertures possess large aberrations.
(b) The mutual repulsion between electrons, due to their charge, causes a tendency for the beam to diverge in the grid-screen region.
(c) The electrons are emitted from the cathode with finite velocities, distributed according to the Maxwell law.

(d) The electrostatic field configuration in the vicinity of the screen grid is such as to deflect the electrons towards the screen wires.

In Appendix I it is shown that the space-charge effect mentioned in (b) above is insufficient to account for observed screen currents, and it can readily be demonstrated (for example, by observing the variation in the proportion of cathode current intercepted by the screen as the cathode temperature is varied) that electron emission velocity is also not a major cause of the spread of the beams. It must therefore be concluded that the screen currents obtained in practice result from the existence of large aberrations in the lenses, from the effect of the electrostatic field in the screen region, or from both these causes.

Now the method employed by Bull to determine the focal length is, as he points out, valid only for electrons travelling close to the central plane AB (Fig. 1). It is clear, however, that the screen current does not arise from these electrons, but from those passing very near to the control-grid wires and we are, therefore, justified in asking whether the focal plane is, in fact, the optimum position for the screen. In view of the difficulty of obtaining an analytical solution for the trajectories of electrons passing near the control-grid wires, involving as it would

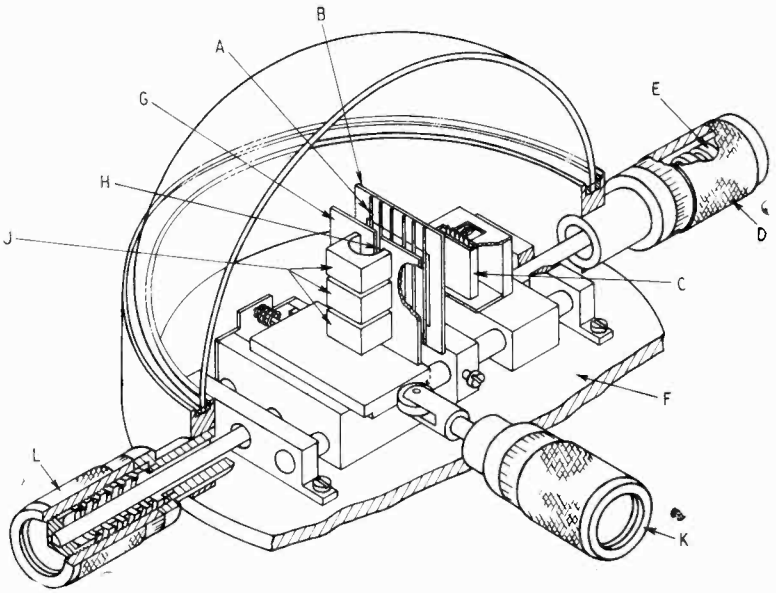

Fig. 2. *Simplified sketch of experimental valve.*

consideration of the effect of space charge on the field in the grid region, it was decided that an experimental approach would be profitable. The investigation to be described here was accordingly undertaken; viz., an investigation of the distribution of current density in the plane of the screen.

This current density distribution depends on the trajectories of individual electrons in their flight from the cathode to the screen plane, and hence on the field configuration in the grid region. It does not depend appreciably on the geometry of the screen, except in the immediate proximity of a screen wire, since the field irregularities do not extend far into the grid-screen space. In making these measurements, details of which are given in a later section, the screen was replaced by a solid metal plate provided with a narrow slot, the current passing through the slot thus being a measure of the current density falling on the plate. The measured distribution is, therefore, that appertaining to a particular cathode-grid geometry and grid-screen distance, and does not include the localized effect around the screen wires. The measurements were carried out for a range of grid-screen distances and with various cathode-grid geometries.

It should be noticed that while this method enables the optimum screen position to be determined, it does not enable the screen current at this position to be predicted. The screen current will, in general, depend on the conditions obtaining in the screen-anode region (e.g., the potential and location of the anode and the space-charge conditions in the intervening space) as well as on the diameter and spacing of the screen wires.

2. Experimental Procedure

The measurements were made on a continuously-evacuated demountable valve in which the electrodes could be moved by manipulation of external micrometer controls while the valve was in operation. In the interests of simplicity attention has been confined to parallel plane electrode structures. However, little error should arise in the application of the results to practical valve designs, since the grid-support rods effectively divide the valve into two sections, each of which approximates roughly to a parallel plane structure.

A simplified sketch of the apparatus is shown in Fig. 2. The grid consisted of straight molyb-

denum wires A welded to a rectangular steel frame B. The cathode C was of the indirectly-heated oxide-coated nickel type, the coated area being a flat face 13 mm × 10 mm. The cathode-grid distance could be adjusted by means of the micrometer screw D. The vacuum was maintained by the flexible metal bellows E soldered to the metal envelope F of the valve.

As mentioned in the introduction, the screen was replaced by a flat metal plate, shown at G in the figure. This plate was provided with a slot H, 0.1-mm wide, parallel to the grid wires, behind which was located a collector electrode J, operated at a positive potential of 150 volts with respect to the anode G. The current flowing to this collector electrode was a measure of the current density falling on the anode plate. The whole plate could be moved in a direction parallel to the grid plane and perpendicular to the grid wires by the micrometer screw K. Thus by observing the variation of the collector current as the slot in the anode was moved from a position behind one grid wire to behind the next, the variation in current density across the electron beam could be determined.

The anode-grid spacing was also variable and was controlled by micrometer L. In order to avoid spurious effects at the ends of the slot, the collector was divided into three sections as shown, and measurements were made of the current to the centre section only, the outer two sections being maintained at the same potential as the centre section. Since under some conditions the current reaching the collector amounted to a few microamperes only out of a total cathode current of 4 mA it was necessary to prevent electrons from reaching the collector by other than the intended paths; for instance, by secondary emission from various parts of the apparatus. This was accomplished by suitably placed shields at cathode potential; these have been omitted from Fig. 2 for the sake of clarity.

The experimental procedure was to scan the beam emerging from the centre grid aperture by moving the collector slot transversely and measuring the collector current at intervals of 0.1 mm. This process was repeated for various anode-grid distances, the total anode current being maintained constant at 4 mA by adjusting the anode voltage. Because of the large number of variables that would otherwise be involved, measurements have been made with the grid at cathode potential only. A curve showing the ratio of the collector current at each point in the beam section to the average across the beam was plotted for each anode-grid distance. This ratio is equal to the ratio of the current density at that point to the average current density. A typical series of such curves is shown in Fig. 3.

It is readily shown that, provided the effects of initial emission velocity are negligible, the shapes of the electron trajectories are dependent only on the shape of the electrodes and not on the actual dimensions. Hence, any geometrical scaling factor can be used without changing the

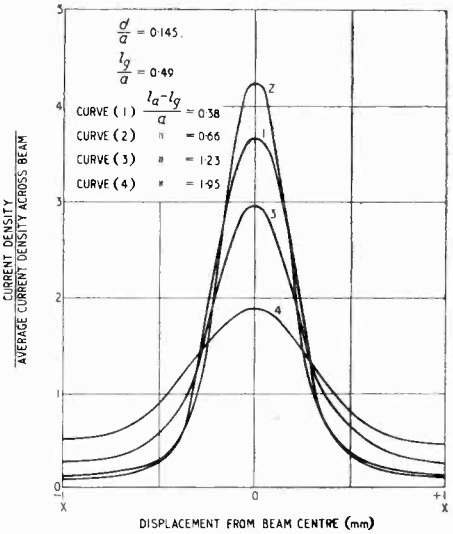

Fig. 3. *Variation in current density across the electron beam.*

relative distribution of current density. It is, therefore, convenient to maintain one dimension constant and to relate the other dimensions to this fixed dimension. In this case the grid pitch a was kept constant at 2 mm and other dimensions were in terms of grid pitch. The experiments were repeated for various values of the ratio l_g/a (cathode-grid distance/grid pitch) and d/a (grid-wire diameter/grid pitch) likely to be encountered in practice. (See also list of symbols).

The shape of the electron paths is dependent also on the ratio only of the electrode potentials and not on their magnitude. However, since the grid was maintained at cathode potential, this amounts to saying that the relative distribution of current density is independent of anode voltage.

3. Results and Their Significance

Referring again to Fig. 3, which shows a typical series of curves of current distribution in the anode plane (or in what would be the screen plane, were the valve a tetrode) it will be seen that, as would be expected, the current density rises from a minimum behind the grid wires to a maximum value midway between them.

These curves were obtained with $d/a = 0.145$ and $l_g/a = 0.49$. As the ratio grid-anode distance/grid pitch, $(l_a - l_g)/a$ is increased, the magnitude

of the maximum between the grid wires rises until it is itself a maximum and then falls again, the maximum in this case occurring when $(l_a - l_g)/a = 0.65$. This is made clearer by reference to Fig. 4, in which the dotted curve shows the variation with $(l_a - l_g)/a$ in current density in the mid-plane between the grid wires; i.e., along the line AB, Fig. 1.

Quite obviously the value of $(l_a - l_g)/a = 0.65$, which gives a maximum in this curve, corresponds to the case when the focus of the electron beam is in the plane of the anode or, of course, the screen, had the valve been a tetrode. It is interesting to note that, with the electrode geometry corresponding to this point, the position of the focus as determined by Bull's method would have been at a distance $0.45a$ from the grid plane.

Now let us examine the variation in current density behind the grid wires, and in the plane of the anode of the experimental triode (i.e., along the line CD, Fig. 1) as the anode-grid distance is varied. This current is given by the points X on the curves of Fig. 3, but is shown more clearly by the solid curve of Fig. 4, which has been plotted from Fig. 3. It will be seen that there is no minimum corresponding to the maximum occurring along AB, but rather that the current density increases progressively as the distance between grid and anode is increased.

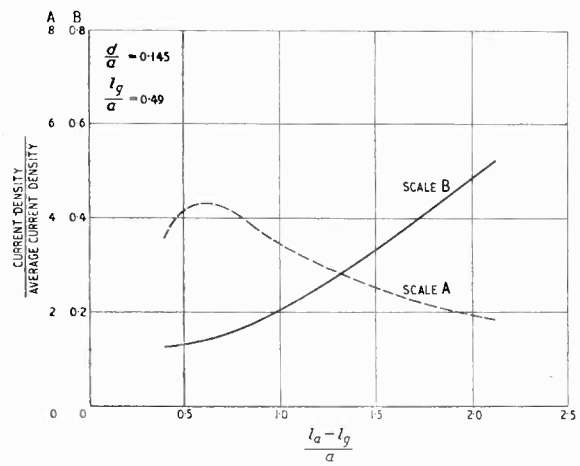

Fig. 4. *Variation of current density along the line AB of Fig. 1 (dotted curve) and along the line CD (solid curve).*

The implication of this is clearly that for minimum screen current, at least at zero grid voltage, the screen should be located as nearly as possible to the control grid, and not in the plane of the focus, as is frequently assumed. However, before considering this point further, the effect of varying the other valve dimensions will be described.

Fig. 5 shows a family of curves similar to those of Fig. 4, plotted for various values of the grid-wire diameter/grid pitch parameter d/a. It will be seen that the value of $(l_a - l_g)/a$ for which the beam focuses in the anode plane decreases as the grid-wire diameter is increased. This

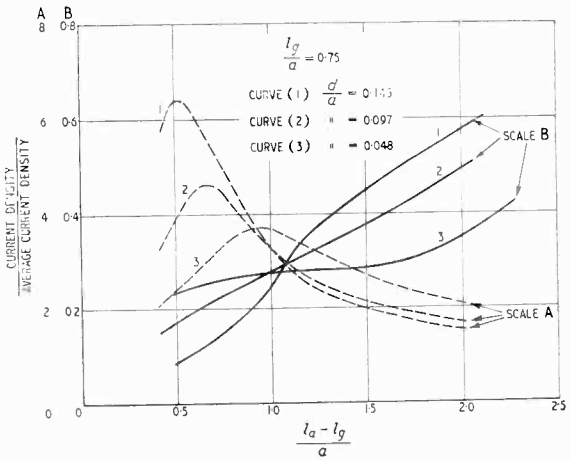

Fig. 5. *Variation of current density along the line AB (dotted curves) and along the line CD (solid curves) for various values of d/a.*

is also shown in Fig. 6, which shows the value of $(l_a - l_g)/a$ for which the beam focuses in the anode plane versus the grid-wire diameter parameter d/a.

The effect on the current density behind the grid wires is, as shown in Fig. 5, that for small values of $(l_a - l_g)/a$ the current density decreases with increasing wire diameter, while for large values of $(l_a - l_g)/a$ the reverse is the case.

Fig. 7 shows another series of curves, also similar to Fig. 4, plotted for a constant grid-wire diameter, corresponding to $d/a = 0.048$ and for varying cathode-grid distances. It will be seen that the value of $(l_a - l_g)/a$ for focus in the anode plane is substantially independent of cathode-grid distance, but that the value of the current density maximum increases as the cathode-grid distance increases. It should be mentioned here that these maxima of current density may be quite appreciably in error, since the measuring slot has finite width, and this width may be greater than the width of the high-current-density part of the beam in cases where the focus is very sharp.

In Appendix II an expression is developed for the focal length of the lens formed by the grid apertures, using a similar method to that used by Bull, but based on electrostatic considerations only. The simplicity of the expression obtained in this way draws attention to the fact that the dominant feature in determining the focal length at zero grid voltage is the ratio of

grid-wire diameter to grid pitch, a fact which is strikingly confirmed by the measurements.

The expression obtained is

$$f = \frac{3}{2} f_o \left[1 + \frac{1}{6} \frac{f_o}{l_g} \right]$$

$$\text{where } f_o = \frac{a}{\pi} \log \frac{a}{\pi d} \quad \ldots \quad \ldots \quad \ldots \quad (1)$$

In Fig. 6 the calculated value of f is plotted as a function of d/a for $l_g/a = 0.75$, the experimental results being shown for comparison. For reasons outlined in the appendix, the apparently good agreement between the calculated and measured values is probably due to a fortuitous cancellation of errors.

The effect of change in cathode-grid distance on the current density behind the grid wires is also shown in Fig. 7. At small values of $(l_a - l_g)/a$ the current density decreases with increase of l_g/a, while with larger values of $(l_a - l_g)/a$, it increases with l_g/a.

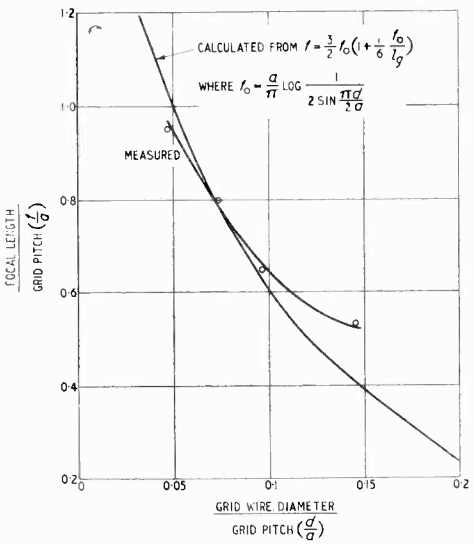

Fig. 6. *Value of $(l_a - l_g)/a$ for which the beam focuses in the anode plane; both curves relate to $l_g/a = 0.75$.*

An interesting series of curves is shown in Fig. 8. These are similar to Fig. 3, and show the current-density distribution across the electron-beam section for thin grid wires. When the anode is very close to the grid [i.e., for $(l_a - l_g)/a$ small] the distribution of current is seen to take the shape of a double-humped curve. This provides additional confirmation, if any is necessary, that the lenses formed by the grid apertures have large aberrations, for it is clear that in this case the outer electrons of the beam are subject to a stronger lens action than those in the centre, resulting in a 'crowding' of electrons at the outer edges of the beam.

Let us now consider whether these results can be applied to the design of a practical valve with reduced screen current. The results apply only to zero grid voltage, of course, whereas in use the valve will normally have an alternating voltage applied to the grid, and it is the average screen current over the grid-voltage cycle which must be minimized. However, if we confine our attention to amplifiers in which the grid is not driven positive, the conditions for minimum average screen dissipation and minimum dissipation at the instantaneous current maximum would not be expected to be very different.

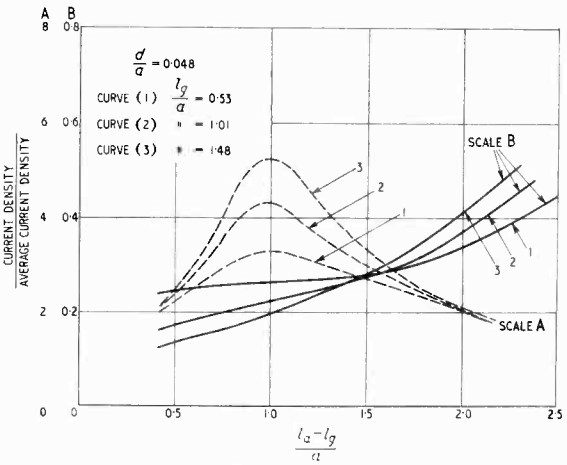

Fig. 7. *Variation of current density along the line AB of Fig. 1 (dotted curve) and along the line CD (solid curves) for various values of l_g/a.*

It is clear from Figs. 3 and 4 that to intercept the minimum cathode current, the screen-grid wires should be as near to the control grid as possible. Reducing the control-grid-to-screen distance will also have the effect of reducing the grid-to-screen amplification factor of the valve, and since, in general, it will be necessary for the static characteristics of the valve to be within specified limits it will be necessary to correct this reduction in amplification factor by increasing the diameter of the grid wires. As shown in Fig. 5, if the grid-screen distance is less than the grid pitch, the effect of large diameter grid wires will be to reduce the screen current still further. Fig. 7 shows that, with large grid wires and small grid-screen distances, the screen current will not vary rapidly with cathode-grid distance, and hence this distance need depend only on the static characteristic requirements.

The limit to the reduction in control-grid-to-screen distance is set by practical considerations. Also, when the cathode-grid distance is small, a

small grid-to-screen distance and large diameter grid wire result in non-uniformity of the field at the cathode and consequent increased curvature of the grid-volts–anode-current characteristics.

It will be appreciated that even if these findings were applicable to positive grid voltages, they would not be of much value. A grid of large diameter wires operated at a positive voltage would itself intercept an intolerably high proportion of the cathode current.

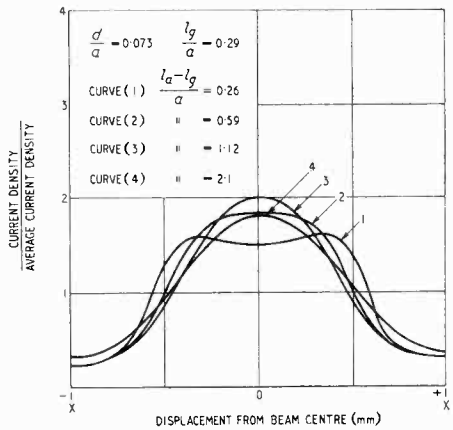

Fig. 8. *Variation of current density across beam section for thin grid wires and small value of l_g/a.*

the current density flowing in the region in which the screen wire is located, and by the shape of the electrostatic field in the immediate vicinity of the screen wire. Spangenberg[4], in a theoretical investigation of the positive-grid triode, has shown that in the case of equal grid and anode voltages the positive grid may be considered to intercept current over an area that normally lies between 1.25 and 1.8 of the projected area of the wire. It is possible that Spangenberg's method could be adapted to give an approximate solution for the tetrode, by considering the tetrode control-grid plane as the cathode of Spangenberg's triode, but since the method is based on electrostatic considerations only, it could not be used when the space-charge in the screen-anode region is appreciable. It could be applied, therefore, only to the case of small screen-to-anode distance and high anode voltage, and would not be valid in the more interesting case of the tetrode in which space-charge in the screen-anode region is used to suppress secondary emission from the anode. Furthermore, the process of treating the control grid as the electron source would be valid only for large grid-to-screen distances, whereas it has been proposed above that the method of reducing screen current is to reduce this distance.

The other component of screen current (viz., that returned from the screen-anode region)

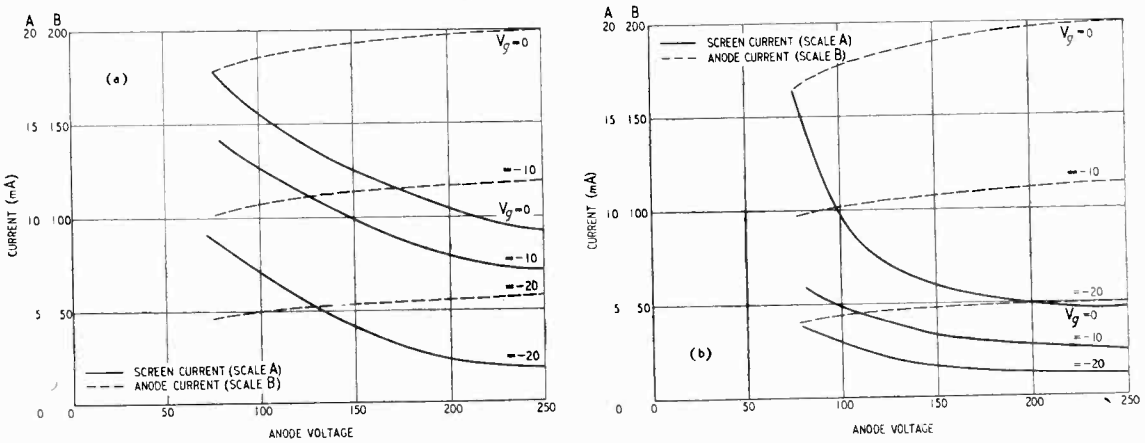

Fig. 9. *Screen and anode currents of (a) valve similar to the Type 807 at 250-V screen-grid potential; (b) valve with thicker grid wires and decreased grid-to-screen distance; screen-grid potential = 200 V.*

Next let us consider whether the results of these experiments can be used to predict the screen current when the valve geometry is known. It is convenient to regard the screen current as consisting of two components, a forward component arriving from the cathode-grid region, and a reverse component consisting of electrons returned from the screen-anode region. The first-mentioned component will be determined by will depend only on conditions existing beyond the screen. In most beam tetrodes this component will predominate only at very low anode voltages, while the first-mentioned component will predominate at high anode voltages. Any improvement effected by reducing the control-grid-to-screen distance will, therefore, be apparent mainly at high anode voltages.

In order to verify the general conclusions

reached, the following experiment was carried out. A valve was made similar to the type 807 beam power tetrode, but in which the ratio screen-grid distance/grid pitch was reduced from 1.49 to 0.58 and the grid-wire diameter was increased such that d/a was 0.192 instead of 0.096 for the normal valve. It was hoped in this way to make a valve having similar characteristics to the 807 in the negative-grid region, but with reduced screen current. In the modified valve, the screen current was 5.0 mA at $V_a = 250$ V, $V_{g1} = 0$, $I_a = 200$ mA. (I_a set to 200 mA by adjusting the screen voltage), compared with 10 mA for the normal valve. Owing to the fact that the increase in grid-wire diameter did not quite compensate for the decrease in grid-screen distance, the anode current of 200 mA was obtained at a somewhat lower screen voltage than normal; viz., 200 V instead of 250 V. This resulted in the space-charge conditions in the screen-anode space being altered with a consequent slight change in the shape of the anode-volts–anode-current curve. The characteristic curves of the modified and the normal valve are shown in Figs. 9(a) and (b) respectively for comparison. In the modified valve, some increase in the curvature of the grid-voltage–anode-current characteristic was noticeable.

4. Conclusion

These experiments have shown that some reduction in the screen current in an aligned-grid valve should be possible by the use of a smaller grid-to-screen distance than is common at present, provided this reduced spacing is not incompatible with conditions set by other characteristics of the valve. This conclusion is in accord with physical reasoning, for it is clear that there must be regions of very low current density immediately behind the control-grid wires, since the only electrons able to reach these regions—apart, of course, from those returned from the screen-anode space at low anode voltages—are those suffering deflections of nearly 90° at the control grid.

5. Acknowledgment

The author wishes to thank Mr. M. T. G. Chick for valuable assistance in the experimental work, and Messrs. Standard Telephones & Cables Limited for permission to publish this paper.

APPENDIX I

Space-charge defocusing.

This appendix is intended to show that defocusing of the electron beams, due to space charge, does not cause appreciable spreading of the beam. It is convenient to consider the case of an aberration-free lens of such focal length that the beam would form a line focus in the plane of the screen in the absence of space-charge. The presence of space-charge will cause the beam to have finite thickness in the screen plane, and it is our aim to find this beam thickness.

An electron will emerge from the grid plane with a velocity v_z given by

$$v_z = \sqrt{\frac{2eV_o}{m}} \qquad (2)$$

where V_o is the effective potential in the grid plane in electrostatic units.

The electron then travels under the influence of an accelerating field towards the anode. This field will be assumed uniform and equal to

$$\mathcal{E} = \frac{V_a - V_o}{l_a - l_g} \text{ electrostatic units} \qquad (3)$$

The distance travelled in time t is

$$\sqrt{\frac{2eV_o}{m}}\, t + \tfrac{1}{2}\frac{e}{m}\frac{(V_a - V_o)\, t^2}{(l_a - l_g)} \text{ cm} \qquad (4)$$

so that the time t_o taken to reach the screen plane is given by

$$(l_a - l_g) = \sqrt{\frac{2eV_o}{m}}\, t + \tfrac{1}{2}\frac{e}{m}\frac{(V_a - V_o)\, t^2}{(l_a - l_g)} \qquad (5)$$

whence

$$t_o = \sqrt{\frac{2m}{e}}\,\frac{(\sqrt{V_a} - \sqrt{V_o})\,(l_a - l_g)}{(V_a - V_o)} \qquad (6)$$

Now the 'half-width' y_t of the beam at time t is given by Thompson and Headrich.[5] Expressed in the symbols used here it is:

$$y_t = y_o - v_y t + 2\pi I v_z \frac{m}{e}\frac{(l_a - l_g)^2}{(V_a - V_o)^2}\left(1 + \frac{(V_a - V_o)et}{v_z(l_a - l_g)m}\right)\left[\log\left(1 + \frac{(V_a - V_o)et}{v_z(l_a - l_g)m}\right) - 1\right] + \frac{2\pi I v_z (l_a - l_g)^2\, m}{(V_a - V_o)^2\, e} \qquad (7)$$

where y_o is the initial 'half-width' of the beam,

I is the current in the beam per cm of beam breadth; i.e., measured parallel to the cathode and to the grid wires,

v_y is the initial velocity of the outermost electrons in a direction perpendicular to the grid wires and to the cathode face.

If the focal length of the lens is such that, in the absence of space-charge, a line focus would be formed in the screen plane,

$$y_o = v_y t_o \qquad (8)$$

Now substituting in (7) for v_z, t_o, and v_y from (2), (6) and (8) and rearranging, we get

$$y_{to} = \frac{2\pi I \sqrt{\frac{2mV_o}{e}}\,(l_a - l_g)^2}{(V_a - V_o)^2}\left\{\frac{\sqrt{V_a}}{\sqrt{V_o}}\left[\log\frac{V_a}{V_o} - 1\right] + 1\right\} \qquad (9)$$

Hence the ratio total beam width/grid pitch

$$= 2y_{to}/a$$

$$= \frac{4\pi J\sqrt{\frac{2e}{m}}\sqrt{V_o}\,(l_a-l_g)^2}{(V_a-V_o)^2}\left\{\frac{\sqrt{V_a}}{\sqrt{V_o}}\left[\log\frac{\sqrt{V_a}}{\sqrt{V_o}}-1\right]+1\right\} \quad (10)$$

where J is the average current density over the cathode surface;

$$\text{i.e., } J = \frac{I}{a} \quad (11)$$

It is well known that

$$J = \frac{\sqrt{2}}{9\pi}\sqrt{\frac{e}{m}}\frac{V_D^{3/2}}{S^2} \quad (12)$$

where V_D is the effective anode potential of the so-called equivalent diode and S is the effective cathode-anode distance of this diode.

The values of V_D and S have been the subject of much discussion. It will be sufficiently accurate here to take

$$V_D = V_g + V_a/\mu \quad (13)$$

and

$$S = l_g + l_a/\mu \quad (14)$$

Substituting for J from (12), (13) and (14) and considering the case when $V_g = 0$, we obtain

$$2y/a = \frac{8}{9\mu^{\frac{3}{2}}}\frac{(l_a-l_g)^2}{(1-V_o/V_a)^2(l_g+l_a/\mu)^2}\left[\left(\log\sqrt{\frac{V_a}{V_o}}\right)+\sqrt{\frac{V_o}{V_a}}-1\right] \quad (15)$$

$\frac{V_o}{V_a}$ can be obtained by Bull's method [1] or, alternatively, from electrostatic considerations only, from Appendix II, equation (17).

For example, when $l_a = 3l_g$

$a = l_g$

$d/a = 0.1$

then $\mu = 10.6$

and $V_o/V_a = 0.0735$

so that $2y/a = 0.042$.

It is thus clear that the beam spread, due to space-charge, is not sufficient to account for the values of screen current observed in practice.

APPENDIX II

Davisson & Calbick's equation for the focal length of a cylindrical electrostatic lens is

$$\frac{1}{f_o} = \frac{\mathcal{E}_2-\mathcal{E}_1}{2V_o} \quad (16)$$

where V_o is the potential in the aperture, and $\mathcal{E}_1$ and $\mathcal{E}_2$ are the fields on the entrance and exit sides of the lens respectively.

The effective potential in the grid-plane of a parallel plane triode at zero grid voltage is given by

$$V_o = V_a\frac{l_g}{l_a+\mu l_g} \quad (17)$$

provided the interelectrode spacings are not small compared with the grid pitch. The relevant values of $\mathcal{E}_1$ and $\mathcal{E}_2$ are those at the cathode and anode, respectively.

$$\text{Hence } \mathcal{E}_1 = \frac{V_o}{l_g} = \frac{V_a}{l_a+\mu l_g} \quad (18)$$

$$\text{and } \mathcal{E}_2 = \frac{V_a-V_o}{l_a-l_g} = \frac{V_a}{l_a-l_g}\left(1-\frac{l_g}{l_a+\mu l_g}\right) \quad (19)$$

From (16), (17), (18) and (19), we obtain after simplification

$$f_o = \frac{2(l_a-l_g)}{\mu} \quad (20)$$

For moderately thin grid wires,

$$\mu = \frac{2\pi(l_a-l_g)}{a\log\frac{1}{2\sin\frac{\pi d}{2a}}} \quad (21)$$

$$\text{whence } f_o = \frac{a}{\pi}\log\frac{1}{2\sin\frac{\pi d}{2a}} \quad (22)$$

In this expression f_o is the focal length of the lens formed by a grid aperture. This focal length is not the distance between the grid plane and the line focus of the beam, however, since, after leaving the lens region, the electrons travel along parabolic paths under the influence of a uniform accelerating field.

The distance f from the lens to the point where the beam focuses is shown by Bull to be

$$f = f_o\left[1+\tfrac{1}{4}\frac{f_o}{(l_a-l_g)}\left(\frac{V_a}{V_o}-1\right)\right] \quad (23)$$

$$= f_o\left[1+\tfrac{1}{4}\frac{f_o}{(l_a-l_g)}\left(\frac{l_a+\mu l_g}{l_g}-1\right)\right] \quad (24)$$

$$= \tfrac{3}{2}f_o\left[1+\tfrac{1}{6}\frac{f_o}{l_g}\right] \quad (25)$$

f/a has been plotted versus d/a for $l_g/a = 0.75$ in Fig. 6, and it will be seen that there is reasonably good agreement with the measured figures. A possible explanation of this unexpected agreement is as follows:—

In calculating f, V_o was taken to be the average potential in the grid plane, whereas the potential mid-way between the grid wires should have been used; this, in the absence of space-charge, would be greater than the average potential. On the other hand, the effect of space-charge would be to reduce the potential between the grid wires, and thus the errors arising from the two sources are seen to be in opposite senses.

REFERENCES

[1] "The Alignment of Grids in Thermionic Valves." C. S. Bull. *J. Instn elect. Engrs*, Part III, June, 1945.

[2] Davisson & Calbick. *Phys. Review*, August 1st, 1931.

[3] Davisson & Calbick. *Phys. Review*, November 15th, 1932.

[4] "Current Division in Positive Grid Triodes," Spangenberg. *Proc. Inst. Radio Engrs*, May, 1940.

[5] "Space-charge Limitations on the Focus of Electron Beams," Thompson & Headrich. *Proc. Inst. Radio Engrs.*, July, 1940.

TRIPLET REFLECTOR ARRAY

By R. W. Hogg, M.A., A.M.I.E.E.

(*Radio Department, Royal Air Force Establishment, Farnborough*)

SUMMARY.—The paper describes a reflector system using parasitic elements arranged in groups of three spaced $\lambda/8$ apart. A theoretical discussion is given, and it is shown that the polar diagrams calculated theoretically are realized with a high degree of accuracy in practice.

Most of the experimental work has been carried out at a wavelength of approximately 6 metres, though the theory is equally applicable to other wavelengths.

In the paper comparisons are drawn between the proposed triplet-reflector arrays and the corresponding arrays having a single reflector element behind each driven element. The relation between reflector reactance required by theory and reflector length found in practice is discussed.

1. Introduction

DURING the development of early-warning radar in the early years of the war, the author took part in the setting up of high-power transmitting aerials. The present suggested design of reflector system arose from a consideration of the difficult problem of minimizing the backward radiation from the transmitting-aerial systems used on the so-called CH radar stations. The object of the design was to obtain a reflector system less sensitive to frequency changes than those already in use and, therefore, demanding less strict tolerances in the cutting of reflector wires to length. Further, it was hoped to secure a better back-to-front ratio than was obtainable using arrays with single reflector elements. It was found, in fact, that no improvement over an array with single reflectors in perfect adjustment (a very critical state of affairs to achieve) was obtained, but that the adjustment of the triplet array was less critical and that the optimum conditions could be realized over a wider band of frequencies.

2. Outline of C.H. and Triplet Arrays

The CH-aerial system was constructed of units consisting of a horizontal half-wave dipole and parasitic reflector spaced 0.17λ apart. The length

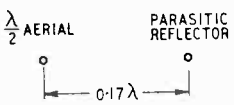

Fig. 1. *Horizontal elements of CH system viewed end on.*

of the reflector was very critical and of the order of $\lambda/2$ (Fig. 1). Such units were stacked vertically at half-wave intervals to form arrays, the number of units in a stack being decided by the wavelength and the height of tower available. In practice this number varied between 4 and 12.

It was suggested that an improvement in performance could be obtained by having three identical reflectors, spaced $\lambda/8$ from one another vertically, behind each 'excited' element (Fig. 2). This is the basis of the triplet system, and these units can be stacked in the same way to form arrays.

MS accepted by the Editor, April 1949

3. Theory of Single Stack Systems

A detailed theoretical treatment of single- and two-stack arrays has recently been given by Walkinshaw.[1] It is only necessary, therefore, to indicate briefly how the polar diagrams of such aerials are calculated in order that the method of calculation might be compared with that used for the triplet array.

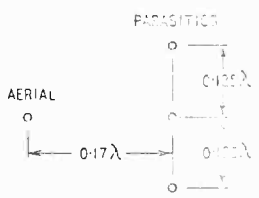

Fig. 2. *End view of triplet reflector.*

3.1 Let us consider first the case of the single $\lambda/2$ dipole and reflector in free space (Fig. 3) where :—

I_0 = current in dipole
I_1 = current in reflector
Z_m = mutual impedance between dipole and reflector
d = distance between dipole and reflector
Z = self-impedance of reflector.

If the e.m.f. induced in the reflector $= I_0 Z_m$

$$I_1 = \frac{-I_0 Z_m}{Z} \text{ and } I_1 Z + I_0 Z_m = 0$$

hence

$$\frac{I_1}{I_0} = -\frac{Z_m}{Z} = A \angle \alpha \text{ say, where } \alpha = \text{angle of lead of } I_1 \text{ on } I_0$$

To calculate the shape of the polar diagram at any distant point P in the plane of the array [Fig. 3(b)], it is convenient to take the aerial current as unity with zero phase angle, and reflector current as $A \angle \alpha$

At P the lead of the reflector current on the aerial current is $\alpha - (2\pi d/\lambda) \cos \theta = \beta$, say.

Then the field at P is proportional to

$$\cos\theta(1 + A\,\underline{/\beta})$$
$$= \cos\theta(1 + A\cos\beta + jA\sin\beta)$$

And the amplitude of the field strength is given by

$$\cos\theta\sqrt{1 + 2A\cos\beta + A^2}$$

The term $\cos\theta$ is used as an approximation to the polar pattern of a half-wave dipole $\frac{\cos(\pi/2\sin\theta)}{\cos\theta}$ and is quite in keeping with the order of accuracy that can be realized from any experimental polar diagrams of backward radiation.

For thin wire half-wave elements Z is taken as $80 + jX$ ohms. A family of polar diagrams can be plotted by altering the value of X; i.e., by varying the length of the reflector. It is found that there is negligible change in the shape of the lobe of forward radiation as X is altered but that the backward radiation changes considerably both in value and lobe shape.

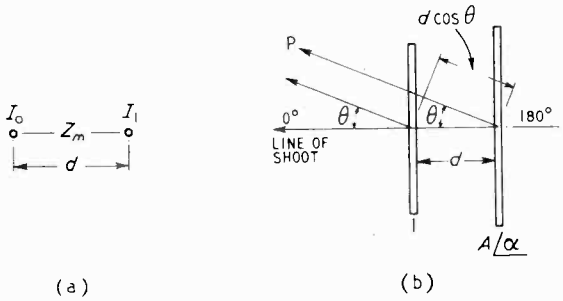

Fig. 3. *Elevation (a) and plan (b) of single dipole and reflector.*

Three polar diagrams have been plotted (see Fig. 4) for X having the values $+40$, $+60$, $+80$ ohms. From the graph of back-to-front ratio versus reflector reactance (Fig. 5), the condition for minimum radiation on the bearing 180° can be seen to occur at $X = 60$ ohms.

3.2 The single-stack triplet-reflector system is treated in the same way as the above.

Let I_0 = dipole current

I_1, I_2 = currents in reflectors

Z_{m1}, Z_{m2}, Z_{m3}, Z_{m4} = mutual impedances between the various elements as shown in Fig. 6.

Z = self-impedance of any of the reflectors (all identical).

By equating the e.m.fs induced in the reflectors

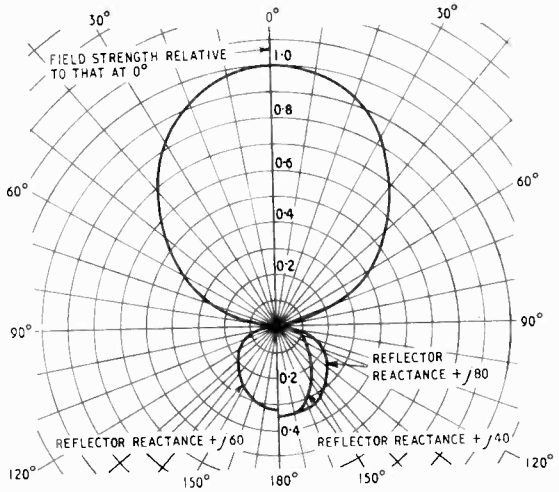

Fig. 4. *Theoretical polar diagram of single-stack array with single reflector.*

to the products of their respective currents and self-impedances, we find that

$$0 = I_0 Z_{m1} + I_1(Z + Z_{m4}) + I_2 Z_{m3}$$
$$0 = I_0 Z_{m2} + 2I_1 Z_{m3} + I_2 Z$$

hence

$$\frac{I_1}{I_0} = -\frac{ZZ_{m1} - Z_{m2}Z_{m3}}{Z(Z + Z_{m4}) - 2Z_{m3}^2} = A_1\,\underline{/\alpha}, \text{ say}$$

and

$$\frac{I_2}{I_0} = -\frac{Z_{m2}(Z + Z_{m4}) - 2Z_{m1}Z_{m3}}{Z(Z + Z_{m4}) - 2Z_{m3}^2} = A_2\,\underline{/\alpha_2}, \text{ say.}$$

Putting $\beta_1 = \alpha_1 - (2\pi d/\lambda)\cos\theta$, and $\beta_2 = \alpha_2 - (2\pi d/\lambda)\cos\theta$

the shape of the horizontal polar diagram is readily seen to be given by the expression

$$\cos\theta\,(1 + 2A_1\,\underline{/\beta_1} + A_2\,\underline{/\beta_2})$$

whose amplitude is

$$\cos\theta\sqrt{(1 + 2A_1\cos\beta_1 + A_2\cos\beta_2)^2 + (2A_1\sin\beta_1 + A_2\sin\beta_2)^2}$$

For ease of numerical evaluation this can be written

$$A_2\cos\theta\sqrt{\left\{\frac{1}{A_2} + \frac{2A_1}{A_2}\cos\beta_1 + \cos\beta_2\right\}^2 + \left\{\frac{2A_1}{A_2}\sin\beta_1 + \sin\beta_2\right\}^2}$$

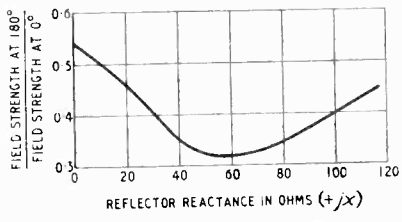

Fig. 5. *Back-to-front ratio of single stack with single reflector.*

Back-to-front ratio versus reflector reactance is plotted in Fig. 7 and three selected polar

diagrams in Fig. 8. As might be expected there is a marked decrease in backward radiation by employing three reflectors instead of one, but more noteworthy is the increase in bandwidth, for nowhere does the backward radiation exceed 0.3 of the maximum forward radiation within the range of reflector reactances + 80 to + 200 ohms. This compares very favourably with the 40-ohm tolerance permissible on the single-stack reflector system to keep the back-to-front ratio down to 0.35.

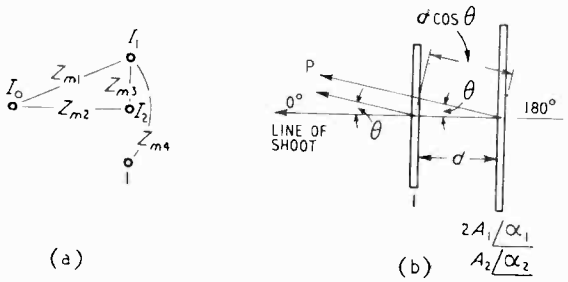

Fig. 6. *Elevation (a) and plan (b) of dipole and triplet reflector.*

4. Two-Stack Arrays

It will be seen from an examination of the polar diagrams calculated by Walkinshaw that the behaviour of two-stack arrays differs in several important respects from that of a single-stack array. The behaviour of arrays with a larger number of elements, however, has been shown to approximate very closely to that of the two stack. Calculations, therefore, have been limited to arrays having two stacks and the comparison which follows is between such arrays having single and triplet reflectors.

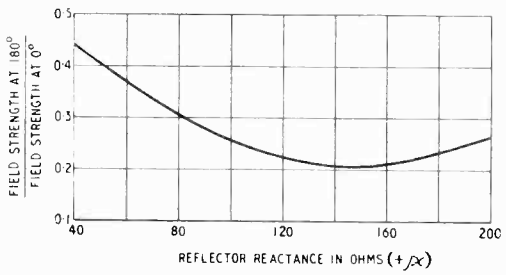

Fig. 7. *Back-to-front ratio of single stack with triplet reflector.*

4.1 *Two-stack Single Reflector Array*

The various currents and mutual impedances are as shown in Fig. 9. Then, as before

$$0 = I_0 Z_{m1} + Z_{m2} + I_1(Z + Z_{m3})$$

hence

$$\frac{I_1}{I_0} = -\frac{Z_{m1} + Z_{m2}}{Z + Z_{m3}} = A\angle\alpha$$

and the field strength at any angle θ (in the horizontal plane) to the line of shoot is proportional to $\cos\theta\sqrt{1 + 2A\cos\beta + A^2}$, where β has the same significance as in Section 3.

Some calculated backward polar diagrams are shown in Fig. 10. The back-to-front ratio deteriorates far more rapidly than for a single-stack array as X deviates from its optimum value (see Fig. 11). For values of X not far off optimum, the ratio is much smaller than can be obtained with a single stack; e.g., a ratio less than 0.12 is maintained over the reactance range $+j40$ to $+j60$ ohms.

Another feature which does not occur with single-stack arrays is the appearance of the so-called 'clover-leaf' pattern, obtained when $X = 40$ ohms. The backward radiation is split into three lobes having equal maxima.

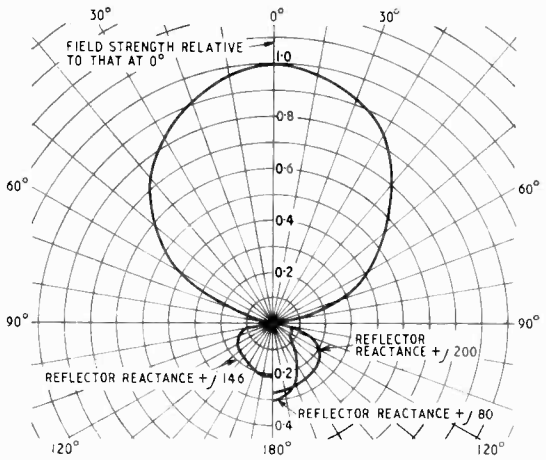

Fig. 8. (Above) *Theoretical polar diagram of single stack with triplet reflector.*

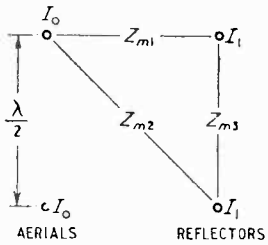

Fig. 9. (Right) *Elevation of two-stack single-reflector array.*

In suppressing backward radiation the field strength at 180° is no longer the only criterion, for once the clover-leaf pattern has been reached any further increase in length (i.e., of inductive reactance) of the reflectors causes the maximum value of the side lobes to rise above the value at 180°.

4.2 *Two-stack Triplet Reflector Array*

The additional reflectors in the triplet system complicate considerably the mathematics involved in calculating the polar diagrams. It is fortunate

that it has been found that multiple-stack arrays approximate very closely as regards polar diagram, to two-stack arrays. Certainly this has only been verified for arrays using single reflectors, but there is no reason to believe that the behaviour would be different for arrays having triplet reflectors. The numerical evaluation of the polar diagram of an array having more than two stacks of triplet reflectors would be extremely complicated and tedious.

The currents, mutual impedances and the vertical spacing are shown in Fig. 12. The other dimensions are as given in Fig. 2.

For reflectors 1, 2 and 3, we find, by equating the induced e.m.fs to the products of the respective reflector currents and self impedances, that :—

$$0 = I_0(Z_{m2} + Z_{m7}) + I_1(Z + Z_{m11}) + I_2(Z_{m3} + Z_{m10}) + I_3(Z_{m4} + Z_{m9})$$

$$0 = I_0(Z_{m1} + Z_{m6}) + I_1(Z_{m3} + Z_{m10}) + I_2(Z + Z_{m9}) + I_3(Z_{m3} + Z_{m8})$$

$$0 = I_0(Z_{m2} + Z_{m5}) + I_1(Z_{m4} + Z_{m9}) + I_2(Z_{m3} + Z_{m8}) + I_3(Z + Z_{m4})$$

For brevity, putting

$$Z + Z_{m11} = B \qquad Z + Z_{m9} = C \qquad Z + Z_{m4} = D$$

$$Z_{m3} + Z_{m10} = E \qquad Z_{m4} + Z_{m9} = F \qquad Z_{m3} + Z_{m8} = G$$

$$Z_{m2} + Z_{m7} = H \qquad Z_{m1} + Z_{m6} = J \qquad Z_{m2} + Z_{m5} = K$$

we obtain from the equations above, the following relationships :—

$$\frac{I_1}{I_0} = \frac{CDH - CKF - DEJ + EGK + FGJ - HC^2}{CF^2 + BG^2 + DE^2 - BCD - 2EFG} = A_1\underline{/\alpha_1}$$

$$\frac{I_2}{I_0} = \frac{BDJ - BGK - DEH + EFK + FGH - JF^2}{CF^2 + BG^2 + DE^2 - BCD - 2EFG} = A_2\underline{/\alpha_2}$$

$$\frac{I_3}{I_0} = \frac{BCK - BGJ - CFH + EFJ + EGH - EK^2}{CF^2 + BG^2 + DE^2 - BCD - 2EFG} = A_3\underline{/\alpha_3}$$

These are shown plotted against reflector reactances in Fig. 13.

Defining the angle θ as shown in Fig. 12(b) ; and β_1, β_2, β_3, by the equations

$$\beta_1 = \alpha_1 - (2\pi d/\lambda)\cos\theta$$

$$\beta_2 = \alpha_2 - (2\pi d/\lambda)\cos\theta$$

$$\beta_3 = \alpha_3 - (2\pi d/\lambda)\cos\theta$$

we find that the field strength at P is proportional to $\cos\theta(1 + A_1\underline{/\beta_1} + A_2\underline{/\beta_2} + A_3\underline{/\beta_3})$.

The amplitude is given by

$$\cos\theta\sqrt{(1 + \Sigma A\cos\beta)^2 + (\Sigma A\sin\beta)^2}$$

Theoretical polar diagrams evaluated by means of this expression are shown in Fig. 14. In general a close similarity exists between these polar diagrams and those of the two-stack single-reflector systems but with this difference : there is a marked increase in bandwidth in the case of the triplet system.

The ratio of the maximum field strength of the largest backward lobe to that of the forward lobe

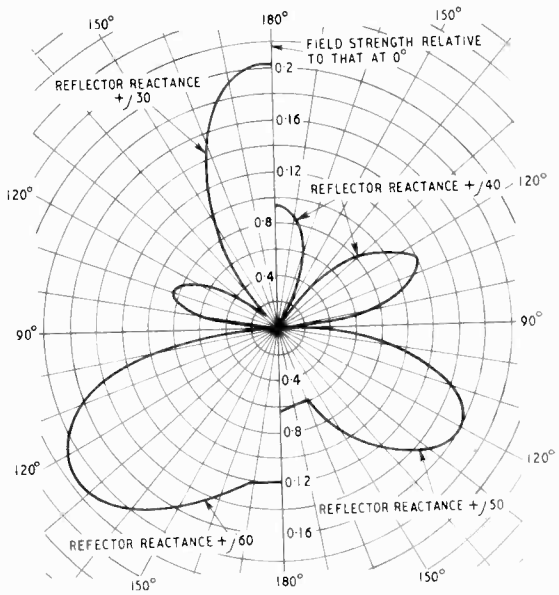

Fig. 10. *Theoretical polar diagrams of two-stack array with single reflectors.*

is less than 0.17 from $j80$ to $j140$ [see Figs. 13(d) and 14]. For the two-stack single-reflector system this ratio is only less than 0.17 between the limits of reflector reactance $j35$ and $j50$, while between the limits $j30$ and $j60$ it is less than 0.2.

The 'clover leaf' patterns are almost identical in the two cases with a back-to-front ratio of about 0.12, the main difference being that a reflector reactance equal to $+j90$ ohms is required for the triplet array whereas $j40$ ohms is required for the array using single reflectors.

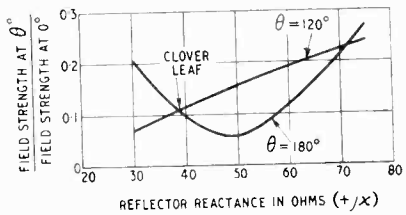

Fig. 11. *Back-to-front ratio two-stack single-reflector array.*

5. Reactance and Length of a Parasitic Element

The question at once arises as to the connection between reflector length and its reactance, for in the construction of an array it is the physical

dimensions that need to be known. Now reflector length can be adjusted experimentally until the polar diagram of minimum radiation at 180° is realized. A further shortening can then be effected so as to obtain the clover-leaf pattern. This change of length, therefore, is equivalent to the difference in reactance given by theory between these two well-defined points. Hence it is possible to work out the non-reactive length of a reflector and also the change of reactance per 1% change in length (referred to $\lambda/2$ for convenience) of reflector.

The results of performing this calculation for the two-stack arrays under consideration is given in Table I.

TABLE I

Type of Two-Stack Array	Non-reactive length	Change of reactance per 1% change in length
Triplet reflector . .	0.48λ	14.9 ohms
Single reflector . .	0.455λ	7.2 ohms

In the arrays used experimentally all elements were made of 200 lb/mile copper wire having a diameter of 0.11 inch. This gives $Z_0 = 800$ approximately for the 6-metre band.

If X is the reactance of an element measured at its centre then $\frac{dX}{d(1/\lambda)} = \pi Z_0$.

whence a reactance change of 12.5 ohms per 1% change in reflector length is quickly evaluated for the case under consideration.

Clearly this reactance change should be a constant for arrays of the same Z_0. The inconsistency of the results may be in part due to the limitations of the sinosoidal theory which assumes that the phase of the current along each wire is constant, a state of affairs which certainly is not true. Good agree-

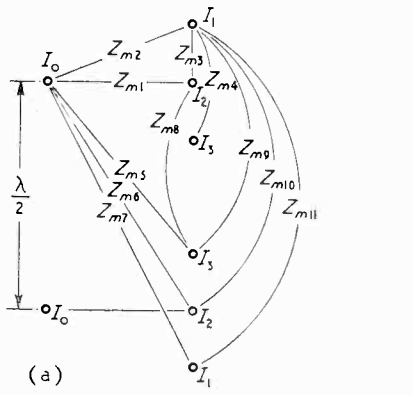

Fig. 12 (above). *Elevation (a) and plan (b) of two-stack triplet-reflector array.*

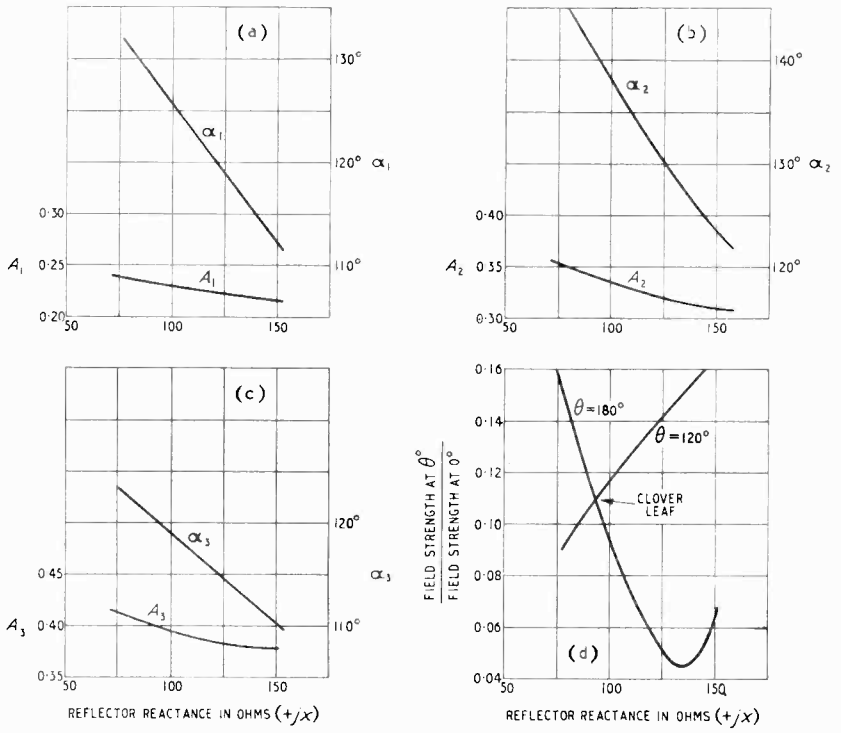

Fig. 13 (right). *Current ratios A_1, A_2 and A_3 and phase angles α_1, α_2, α_3 of two-stack triplet-reflector array are given in (a), (b) and (c), with the back-to-front ratio in (d).*

It is interesting to compare these results with those given by ordinary line theory. Z_0, the characteristic impedance of a parasitic element, can be expressed by the formula :—

$$Z_0 = 120\left[\log_e\left(\frac{l}{a}\right) - 1\right]$$

where l = length of reflector

and a = radius of reflector wire or tube.[2]

ment however, between theory and practice in this respect has been obtained in the case of aerials made of tubing; i.e., having a much lower value of Z_0.[3]

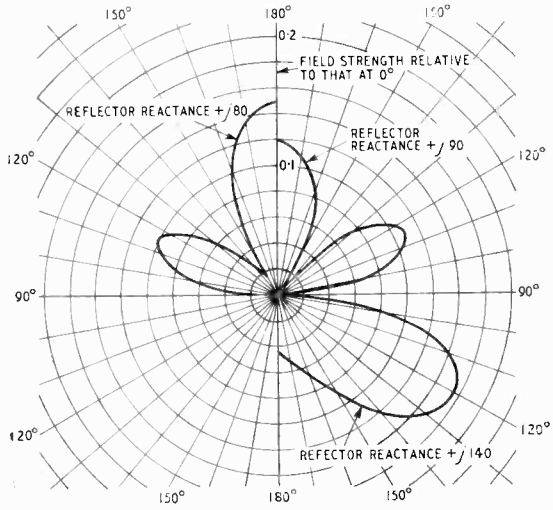

Fig. 14. *Theoretical polar diagram of two-stack triplet-reflector array.*

6. Experimental Work

A two-stack triplet-reflector array constructed from 200 lb/mile copper wire was rigged at a mean height of about 30ft, on a light wooden tower erected on a flat site. Effective shortening of the reflectors due to insulators was avoided by bending small hooks at the ends of the wire elements and tensioning them in position with fine string.

A five-watt c.w. transmitter was used to energize the array and reception was carried out at points round a circle 80 yards in radius, using a horizontal half-wave dipole mounted on a pole about 0.6λ above ground. The array was constructed for a nominal wavelength of 5.9 m, reflector length was 3.01 m($\equiv 0.51\lambda$), and horizontal spacing between dipoles and reflectors was 0.17λ. Vertical spacing between dipoles was, of course, $\lambda/2$.

It will be noticed here that the approximation was made of comparing these experimental polar

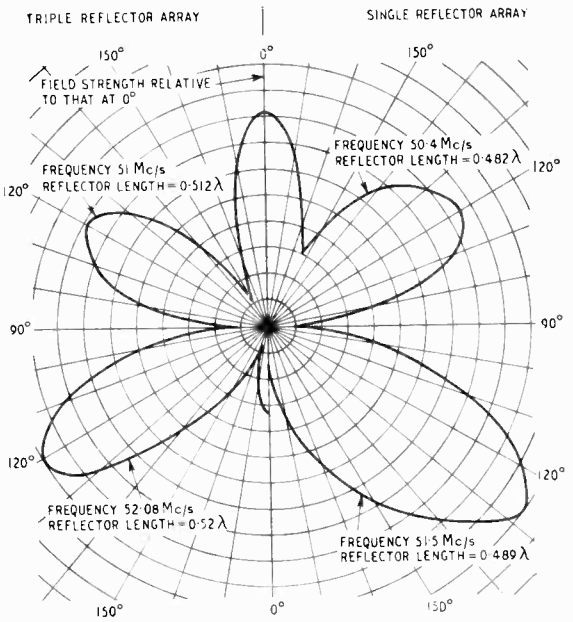

Fig. 15. *Experimental polar diagrams, the arrays being at a mean height of $3\lambda/2$ above ground. For the single reflector the reflector length was 0.487λ and other dimensions were as in Figs. 1 and 3 when $\lambda = 5.9$ m. For the triplet, when $\lambda = 5.9$ m, the reflector length was 0.51λ and the other dimensions were as in Figs. 2 and 12.*

diagrams with those calculated for the aerial system in free space. This is done to avoid unwieldy complications to the theory, and should not involve big errors in practice because

(a) the height of the experimental aerial system above earth was sufficient to render mutual coupling with its images relatively small,

TABLE II

Type of Array	Frequency of Polar Diagram (Mc/s)	Back (180°) to Front (0°) Ratio of Signal Strength		Reflector Length	Reflector Reactance Theoretical (Ω)	Change in React. per 1% change in length (based on $\lambda/2$) (Ω)
		Theoretical	Experimental			
Two-stack Triplet Reflector	51 (clover leaf)	0.122	0.17 approx.	0.512λ	$+j90$	14.0
	52.08	0.044	Not measured	0.52λ	$+j120$	
Two-stack Single Reflector	50.55 (clover leaf)	0.123	0.17 approx.	0.482λ	$+j40$	7.2
	51.5 (min. 180°)	0.062	0.04	0.489λ	$+j50$	

(b) the distance between transmitting and receiving aerials was sufficient for expecting reasonable correspondence between the horizontal polar diagrams measured and those calculated for free-space conditions.

Polar diagrams in a back quadrant were measured at :

(1) 52.08 Mc/s, which was expected to represent minimum 180° radiation, but from the presence of the small lobe at 180° (see Fig. 15) appears to be 0.5 Mc/s low in frequency;

(2) 51 Mc/s, which is the clover-leaf pattern.

A measurement of back-to-front ratio was also made at this frequency.

Results are given in Table II together with those obtained for the single-reflector two-stack system by way of comparison ; the polar diagrams are plotted in Fig. 15. From these results the bandwidth comparison given in Table III for two-stack arrays at the nominal wavelength of 5.9 metres was calculated.

TABLE III

Type of Array	Frequency Shift (Mc/s)	Altering polar Diagram pattern		Equivalent change in Reflector length to give same alterations (cm)
		From	To	
Two-stack Triplet Reflector	1.5	Clover leaf	Min. 180° radiation	9
Two-stack Single Reflector	1	Clover leaf	Min. 180° radiation	5.9

7. Conclusion

Theory would indicate that, for a given standard of performance, the bandwidth of the triplet system should be well over twice that of the ordinary single reflector system, but the experimental evidence available did not bear this out. Whereas, the change in reflector reactance per 1% change in length was, in the case of the triplet-reflector array, not far removed from the theoretical value of 12.5, it was, in the case of the single-reflector system, little more than half this theoretical value. Further experimental work might throw light on this discrepancy but as it stands the triplet shows an increase in bandwidth of the order of 50% over the single-reflector system, or, putting in figures at $\lambda = 6$ m, a workable band of 3 Mc/s as opposed to 2 Mc/s for a two-stack array of the single-reflector type.

8. Acknowledgments

The work which forms the subject matter of this paper was carried out by the author at the Telecommunications Research Establishment as part of the wartime research programme of the Ministry of Aircraft Production. Acknowledgments are due to the Chief Scientist, Ministry of Supply, for permission to publish the paper.

REFERENCES

[1] Walkinshaw, W. "Theoretical Treatment of Short Yagi Aerials," *J. Instn elect. Engrs*, Vol. 93, p. 598, 1946.

[2] Schelkunoff, S. A. "Theory of Antennae of Arbitrary Size and Shape," *Proc. Inst. Radio Engrs*, 1937 Vol. 25, p. 78.

[3] Smith, R. A., and Holt Smith, C. "Elimination of Errors from Crossed Dipole Direction Finding Systems," *J. Instn elect. Engrs*, 1946, Vol. 93, p. 579.

FIXED H-ADCOCK DIRECTION FINDER FOR V.H.F.

By B. G. Pressey, Ph.D., M.Sc.(Eng.), A.M.I.E.E. and G. E. Ashwell, B.Sc.

(Communication from the National Physical Laboratory)

SUMMARY.—The paper describes an investigation into the practicability of the fixed type of H-Adcock direction finder for use at very high frequencies (30-100 Mc/s) under conditions in which the aerial system is remote from the operator. The experimental equipment consisted essentially of two crossed H-Adcock aerials mounted on a wooden tower 10 m high. The aerial system was connected by r.f. transmission lines to a goniometer and receiver situated in a hut near the base of the tower. By making adjustments to the length of the transmission lines and their point of connection to the aerial feeders a high instrumental accuracy was obtained on signals of mixed as well as vertical polarization. The sensitivity was such that bearings with a silent swing of $\pm 5°$ could be taken on field strengths varying between 0.5 and 14 μV/m over the frequency range.

1. Introduction

FOR many applications of v.h.f. direction finders it is important that the aerial system should be situated at some distance from the operator. One particular group of applications is that in which the aerials must be erected at an appreciable height above ground level in order that they shall be clear of obstacles on the site which would seriously impair their performance. A direction finder on board ship is a specific example. It was the use of the H-Adcock system in such cases which was the object of the investigations described in this paper.

At the time when this work was started (June 1942) the Adcock systems which had been developed for this frequency range were of the rotating type.[1] For several reasons, such as the serious effect of wind resistance and moment of inertia of the aerials on the performance of the remote driving arrangements, this type of direction finder was considered unsuitable for the present application. An investigation was therefore made into the practicability of the fixed aerial type erected in an elevated position at a distance of 20 m or more from the operating point.

The experimental system described consisted essentially of two crossed H-Adcock aerials mounted on the top of a 10-m wooden tower. The aerials were connected by r.f. transmission lines to a goniometer and receiver situated in a hut near the base of the tower. The frequency range was limited by the receiver to 27-85 Mc/s.

2. Description

2.1 *Aerial System.*

The aerial system was supported on a wooden framework which was mounted in the centre of a platform at the top of the tower. Each of the two aerial pairs consisted of two vertical dipoles 1.6-m long, spaced 1-m apart and interconnected by a screened horizontal feeder. Dipoles having a cross-sectional area large compared with their length were used so as to reduce the variation of their impedance with frequency. The diameter was 9 cm giving a ratio of diameter to length of 0.055. The resonant frequency was 73 Mc/s. The horizontal feeders consisted of two concentric r.f. cables of 70-Ω characteristic impedance and 2.6 m in length. When the system was first erected the cables were made as short as possible (1.2 m) but it was found that the natural resonance of the aerial pair occurred within the operating frequency range. Satisfactory operation was impossible in the region of this resonance and it was necessary to lengthen the feeders so that the resonance occurred outside the range at a frequency of approximately 27 Mc/s.

The transmission lines from the aerial system to the receiver consisted, like the horizontal feeders, of a pair of 70-Ω concentric cables and were 23 m long. The lines were connected directly to the mid-points of the feeders in the manner shown in Fig. 1. In order to facilitate the adjustment of the actual point of connection when balancing the aerial system, the central portion of the feeders consisted of two thick brass wires bent into semi-circles and mounted on either side of a block of insulating material as shown in Fig. 2. The diameter and spacing of the wires were so chosen that the characteristic impedance of the feeders was maintained. Connection of the lines to these wires was effected through two rotatable contact arms. The lower ends of the lines terminated on the field-coil terminals of the goniometer and a 200-Ω resistor, centre-tapped to earth, was connected in parallel for the purpose of damping line resonances.

MS accepted by the Editor, June 1949

The cables used for the feeders and lines had lead sheaths which were carefully bonded to each other and earthed at the foot of the tower.

2.2 *Goniometer.*

The goniometer was of the inductive type with electrostatically-screened field coils and a relatively high coupling factor. A full description of the instrument and of its performance is given elsewhere.[2]

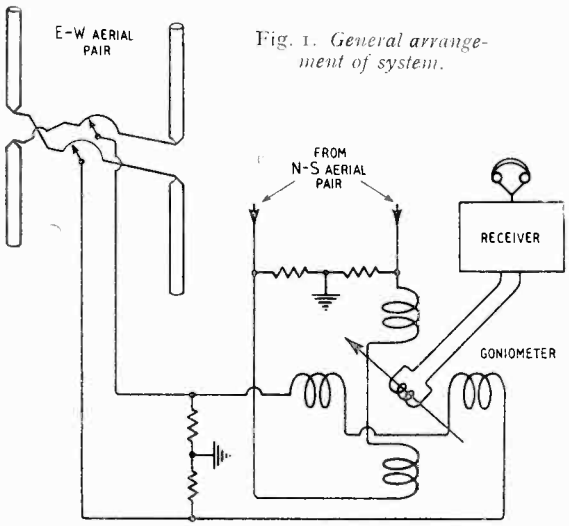

Fig. 1. *General arrangement of system.*

2.3 *Receiver.*

The receiver was a commercial type, the Plessey RL85, covering a frequency band of 27-85 Mc/s in three ranges. Certain improvements to the screening were found to be necessary in order to reduce stray pick-up. The goniometer search coil was connected by a length of twin screened cable ($Z_0 = 100\ \Omega$) to the range switch in the grid circuit of the first r.f. stage and was made as short as possible so as to avoid any resonance of the search-coil circuit within the operational frequency band.

3. Aerial Balance Adjustments

Although the aerial system was constructed to be mechanically symmetrical and the transmission lines were cut to equal lengths, the electric symmetry and equality were not correspondingly good. It was necessary, therefore, to make adjustments to the aerials and the lines in order that the system should give the optimum performance. The adjustments may be conveniently divided into two sections, those for the reduction of 'antenna effect' and those for the reduction of polarization error.

3.1 *Reduction of Antenna Effect.*

Measurement of the antenna effect of each aerial pair was made with the aid of a transmitter with a short vertical aerial. The transmitter was set up on a portable tower at a distance of about 5 m from the direction finder and at the same height. This arrangement was adopted so as to minimize site errors which were appreciable when the transmitter was placed on the ground at a distance of 40 m. The transmitter aerial was set carefully on a line normal to the plane of the aerial pair under examination. The error in bearing was measured over the frequency range at intervals of 1 Mc/s and plotted against frequency. A typical curve for a well-balanced system is shown in Fig. 3. The error curve has two principal components, one varying slowly with frequency, as indicated by the broken line, and the other having the form of rapid fluctuations with a period of between 2 and 4 Mc/s. The former component is due mainly to asymmetry of the aerial pair and the latter to unbalance in the transmission line.

The aerial adjustments for the reduction of antenna effect were made in two stages; first, to the lengths of the line cables, and secondly to the position of the point of connection of the lines to the feeders.

When the direction finder was originally set up screened twin cables were used for the line and the error curve fluctuations were found to be of the order of 5° in 1 Mc/s. By the addition of balancing impedances between the conductors and the sheath of the cable at its lower end it was possible to reduce this error to reasonable proportions at a particular frequency but the

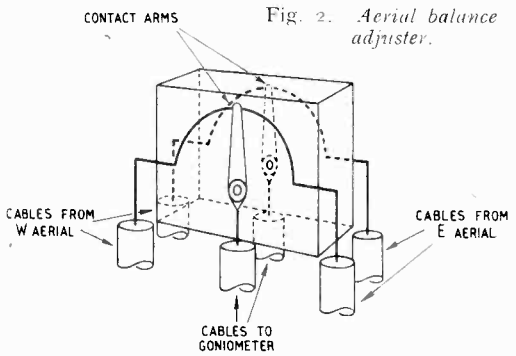

Fig. 2. *Aerial balance adjuster.*

balance did not hold at other frequencies. The substitution of two concentric cables in place of the twin cable enabled the relative lengths of the two cables to be adjusted by cutting until the amplitudes of the error fluctuations were reduced over the whole frequency range to the order of those shown in Fig. 3.

Aerial balance was achieved by moving the two line tapping points together along the feeders until the electrical centre point was found. The adjustment was most critical at

frequencies near the resonance of the aerial pair (27 Mc/s), a movement of 1 mm causing a change of about 1° in the bearing error. Thus adjustment for minimum error on a frequency in this region produced the most satisfactory balance throughout the range.

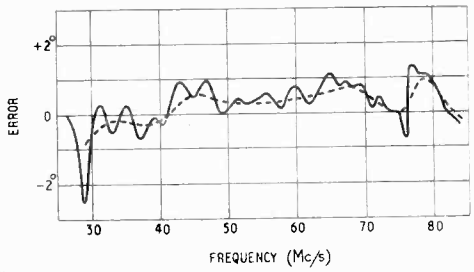

Fig. 3. *Variation of aerial balance with frequency for N–S aerial pair. Full line = measured errors; broken line = mean errors curve.*

3.2 *Polarization Error*

In order to minimize the horizontal pick-up of the aerials it is necessary that the aerials be electrically symmetrical about the horizontal plane containing the feeders. This symmetry was obtained by further adjustment of the connection points of the lines to the feeders in the same manner as has been used on h.f. direction finders.[3]

As in the case of the antenna-effect adjustments the aerial pairs were balanced in turn using a local transmitter sited on the line normal to the plane of the aerial pair. The transmitter had a dipole aerial capable of rotation in the vertical plane parallel to that of the d.f. aerials. Thus it was possible to introduce a horizontally-polarized component into the incident wave and measure the resultant change in bearing and swing. The dipole aerial was situated at a height of 4 m above the ground and at a distance of 46 m from the direction finder. Measurements over the frequency range showed peak values at 73 Mc/s (dipole resonance) and at 27 Mc/s (aerial-pair resonance), the latter being considerably greater. Accordingly, the two connection points of the lines were moved in opposite directions along the feeders, their mean position (controlling the antenna effect) remaining the same, until the error and swing at this frequency reached a minimum value. The adjustment was as critical as that for antenna effect, the error changing at a rate of approximately 2°/mm.

When the adjustments had been completed for both antenna effect and polarization error the contact arms were soldered in position to prevent further movement and to ensure a good contact.

3.3 *Balance Between Aerial Pairs*

When each aerial pair had been separately balanced it was necessary to make a further adjustment so that the terminal voltages of the two transmission lines should bear the correct relation to each other. For this purpose the test transmitter was set up as for the antenna-effect adjustments but at 45° azimuth. Short lengths were then cut off both cables of one of the lines until the rapid fluctuations in the bearing error/frequency curve reached minimum amplitude.

4. Performance Measurements

When all adjustments to the aerials and lines were finished, complete measurements of the instrumental accuracy and sensitivity were made.

4.1 *Instrumental Accuracy*

A bearing calibration of the direction finder for vertically-polarized waves was made at frequencies of 31, 45, 60 and 80 Mc/s. The test transmitter was set up at a distance of 5 m in the same manner as for the balance adjustments and the d.f. aerial system was rotated in steps of approximately 11°, readings of bearing being taken at each position. For the reason explained below, it was decided to eliminate the effects of the rapid fluctuations of bearing with frequency, by making measurements on a group of three frequencies separated by 1 Mc/s and centred on each of the frequencies stated above. The mean value of the three readings was used in plotting the error curves, two of which, those for 31 and 60 Mc/s, are shown in Fig. 4.

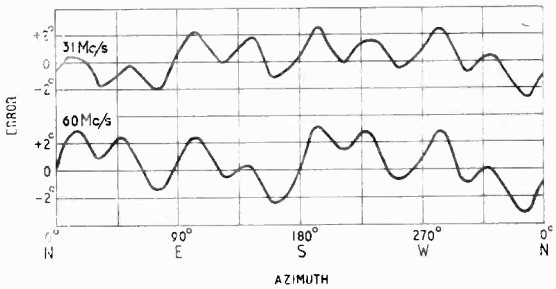

Fig. 4. *Measured calibration curves.*

As stated in Section 3.1, the reason for locating the transmitter very close to the direction finder was the elimination of site error. It is possible, however, to introduce calibration errors due to the proximity of the transmitter, the magnitude of which have been examined by Ross.[4] It can be shown that in the present case the principal error is octantal having a maximum value of about ± 0.2° over the whole frequency range.

The total errors indicated by the curves of Fig 4 are the sum of the errors due to aerial spacing, aerial unbalance, line asymmetry and goniometer imperfections. The maximum value of the octantal-spacing error varied from 0.3° at 30 Mc/s to 1.8° at 85 Mc/s and the goniometer

errors at 31 and 60 Mc/s are shown by the full-line curves of Fig. 5.

Subsequent to the making of these calibrations, considerable improvements in goniometer performance were effected as indicated by the broken line curves of Fig. 5. Unfortunately it was not possible to repeat the calibrations, in order to determine whether there was an overall improvement, but an examination of Figs. 4 and 5 will show that, had this been possible, smoother calibration curves would have been obtained.

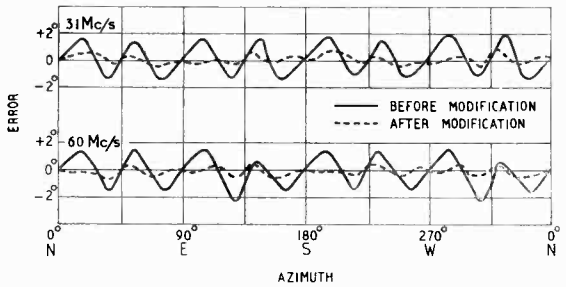

Fig. 5. *Goniometer error curves.*

The method which has been used in obtaining the above calibrations effectively eliminates the rapid fluctuations of error with frequency which are evident in Fig. 3. Examination of this curve shows that in general it would be impracticable to correct for this error on account of the large number of correction curves which would be required. Under special conditions of operation, such as operation over a limited sector of frequency range, however, the use of complete correction curves might be practicable. But, for normal operation of the direction finder, the presence of these rapidly fluctuating errors must be accepted and correction made only for the slowly varying errors. From measurements made during the course of development it is possible to estimate the limit of accuracy due to this uncorrected error for various types of transmission line. Thus, Table 1 shows the highest accuracy which can be expected under various line conditions.

TABLE 1

Transmission-Line Condition	Limiting Accuracy
Twin cable mechanically equal lengths	$\pm 6^\circ$
Pair of concentric cables, mechanically equal lengths	$\pm 4^\circ$
Pair of concentric cables, cut to electrically equal lengths before installation	$\pm 2^\circ$
Pair of concentric cables, balanced in situ	$\pm \frac{3}{4}^\circ$

The error of the direction finder for a wave containing a horizontally-polarized component was measured in the manner described in Section 3.2 with the transmitter placed in line with each aerial pair in turn. From the measured bearing error and swing the total polarization error (i.e., the maximum error obtained when the horizontal and vertical components have the appropriate phase relations) was calculated in the manner already described in a previous paper by one of the authors.[5]

The set up of the transmitter was such that the ratio of the horizontal and vertical components of the field at the d.f. aerials, which had been measured prior to the installation of the aerial system, varied between 5 and 6 over the frequency range. In order to express the results in a rational manner the measured errors were converted to the values which would be obtained with a wave arriving in a horizontal direction and having a ratio of horizontal to vertical field components of unity. The total error under these conditions and with the transmitter in line with one aerial pair is shown in Fig. 6. The small peak value at 72 Mc/s and the high values below 30 Mc/s are associated with the dipole resonance and the aerial-pair resonance respectively. The average error of 0.4° corresponds to a ratio of horizontal to vertical pick-up factors of 0.007.

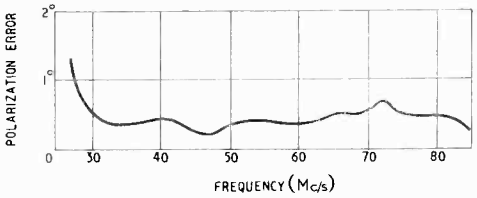

Fig. 6. *Variation of polarization error with frequency for E–W aerial pair. Angle of polarization = 45°; angle of incidence = 90° to vertical.*

4.2 *Sensitivity*

The overall sensitivity of the system is expressed in terms of the field strength of a c.w. signal on which a bearing could be taken with a silent swing of $\pm 5^\circ$, an audible output being obtained by using the internal beat oscillator of the receiver. A transmitter with a vertical aerial provided a signal of known field strength at the d.f. aerials. Only one aerial pair was used for this measurement, the transmitter being set up in line with it, and by connecting a signal generator to the unused goniometer field coil it was possible to inject into the receiver a voltage equal to that produced by the radiated field. By reducing the generator output until just sufficient for a bearing with a $\pm 5^\circ$ swing to be taken, the level of the minimum field strength

relative to that actually incident on the aerials was determined. The measurements were made at intervals over the frequency range and the results are plotted in Fig. 7. The large increase in sensitivity at 70 Mc/s is due chiefly to the improved impedance match between dipoles and feeders at the resonance of the former.

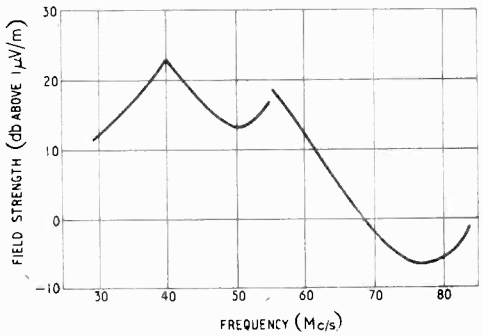

Fig. 7. *Field strength of c.w. signal for ± 5° silent swing.*

5. Operational Performance

The equipment has been operated on routine observations of signals from c.w. and pulse transmitters at distance of 6 to 100 km with satisfactory results.

As the main purpose of the investigation was the development of the equipment and the determination of its performance as an instrument, no great care was taken in choosing a site that would be suitable for observations on distant transmitters. Thus it was found that when taking bearings in connection with the above observations appreciable site errors were present. For instance, the bearing of a transmitter 6 km distant showed a variation with frequency of 2°–3° and varied at a rate of up to 2½° for a frequency change of 0.1 Mc/s. With transmissions on 47 Mc/s from a distance of 35 km the bearings showed a variation of 9° for a frequency change of 1.0 Mc/s. Even on a good site, the errors due to the site will rarely be less than about 1° to 2°, so that the instrumental accuracy which has been achieved is quite adequate in practice.

6. Conclusions

The development of the direction finder and the investigation of its performance has shown that the fixed type of H-Adcock system may be considered a practical v.h.f. system capable of operation over a wide frequency range with a high order of accuracy. It can be made simple in operation having only receiver adjustments apart from the goniometer operation. The initial balancing of the aerial system and transmission lines is rather critical if the greatest accuracy is required but if a maximum probable error of the order of 2° is satisfactory the balancing processes can be considerably simplified.

7. Acknowledgment

The work described above was carried out as part of the programme of the Radio Research Board. This paper is published by permission of the Director of the National Physical Laboratory, and the Director of Radio Research of the Department of Scientific and Industrial Research.

REFERENCES

[1] R. L. Smith-Rose and H. G. Hopkins "Radio Direction Finding on Wavelengths between 6 and 10 metres (Frequencies 50 to 30 Mc/s)" *J. Instn elect. Engrs*, 1938, Vol. 83, p. 87.

[2] B. G. Pressey "Radiogoniometers for High and Very High Frequency Direction Finding" *J. Instn elect. Engrs*, 1948, Vol. 95, Pt. III, p. 210.

[3] B. G. Pressey "A Rotating H-Adcock Direction Finder for High Frequencies" *Wireless Engineer*, 1949, Vol. 26, p. 85.

[4] W. Ross "The Calibration of Four-Aerial Adcock Direction Finders," *J. Instn elect. Engrs*, 1939, Vol. 85, p. 192.

[5] B. G. Pressey "A High Frequency Transmitter for the Measurement of Polarization Error of Direction Finders," *Wireless Engineer*, 1949, Vol. 26, p. 124.

INSTITUTION OF ELECTRICAL ENGINEERS

The following meetings will be held at the I.E.E., Victoria Embankment, Savoy Place, London, W.C.2, commencing at 5.30 :—

Feb. 13th, Discussion meeting on "Interference Suppression," opened by E. M. Lee.

Feb. 15th. "Ground-Wave Propagation over an Imhogeneous Smooth Earth—Experimental Evidence and Practical Implications," G. Millington and G. A. Isted.

Feb. 27th. Discussion Meeting on "Mobile Radio Power Packs," opened by Air Commodore R. L. Phillips, O.B.E.

Mar. 6th, Discussion Meeting on "The Place of High-Frequency Heating in Industry," opened by C. E. Eadon-Clarke.

Mar. 7th. "The Fundamental Limitations of Second-Harmonic Type of Magnetic Modulator as applied to the Amplification of Small D.C. Signals," by Professor F. C. Williams, O.B.E. and S. W. Noble, and "A New Theory of the Magnetic Amplifier," by A. G. Milnes.

BRITISH INSTITUTION OF RADIO ENGINEERS

During February the following meetings will be held :—

London Section, 3rd Mar., at 6.30 p.m., at the London School of Hygiene & Tropical Medicine, Keppel St., W.C.1. ; "Travelling Wave Tubes," by R. L. Kompfner.

West Midlands Section, 1st Mar., at 7 p.m., at the Wolverhampton & Staffordshire Technical College, Wulfruna St., Wolverhampton ; "Electronics and the Brain," by H. W. Shipton.

North Eastern Section, 15th Feb., at 6 p.m., at Neville Hall, Westgate Rd., Newcastle-on-Tyne ; "Single Sideband Systems Applied to Long Range Wireless," by Major S. R. Rickman.

ELECTRON TRANSIT TIME

Effect on Negative-Grid Oscillators

By S. K. Chatterjee, M.Sc., M.I.R.E., and B. V. Sreekantan, M.Sc., A.M.I.R.E.

(Department of Electrical Communication Engineering, Indian Institute of Science, Bangalore, India)

SUMMARY.—Electron transit-time effects on the output and efficiency of some triodes having different geometrical structures have been studied. The results indicate that for valves 833-A, 834, 304-B, the limit of oscillation is reached when the period of oscillation is nearly four times the total time of transit of the electrons from cathode to anode, whereas for valves 316-A, 955, the limiting frequency is reached when the period of oscillation is nearly three times the total time of flight. The transit-time expression given by Gavin[1] has been modified by taking into consideration the alternating voltages on the anode and grid and the negative bias. The wavelengths at which the efficiencies of valves drop by 10% and also down to 10%, have been found and the results compared with values obtained theoretically from the expression given by Gavin.[1]

Introduction

THE highest frequency at which a valve can generate spontaneous oscillation is restricted by the time of flight of electrons from cathode to anode, the interelectrode capacitances and the lead inductances within the valve. When the time required by an electron to travel from cathode to anode becomes comparable with the period of a cycle of oscillation to be generated, the valve performance is modified in a fundamental way and the entire behaviour needs clarification in the light of basic considerations. Electron transit-time increases the effective grid-cathode conductance proportional to the square of the frequency and hence decreases the effective Q of the resonant circuit. At these frequencies the phase relation between anode current and grid voltage is no longer that existing at low frequencies. So the phase angle of the mutual conductance is also affected. A considerable amount of work has been done by Scheibe,[2] Llewellyn,[3], North,[4] Benham,[5] and McPetrie,[6] to evaluate the effect of electron transit time on the assumption that a steady-state space-charge distribution has been established and the high-frequency signal is merely a perturbation, small in comparison with the steady-state component. As remarked by Llewellyn[7] such investigations are inadequate for the case of large signals encountered in power amplifiers and oscillators operated in the class C condition. Expressions which can be used to analyse the type of signals involved in class C operation, have been derived by Chao-Chan-Wang.[8]

The time of electron flight for valves having plane and cylindrical electrodes has been calculated by Fortescue[9] and Kompfner.[10] Assuming that for $r_a/r_g < 3$ and $r_g/r_k < 2$, where r_a, r_g, and r_k represent radii of anode, grid and cathode respectively, plane electrodes may be considered as giving values of transit time which agree within 12% with the values for cylindrical electrodes. Gavin[1] has shown that the time of flight from cathode to anode is given by the following expression

$$\tau = \frac{\sqrt{\mu}}{5.93 \times 10^7 \sqrt{E_{HT}}}\left(3d_{kg} + \frac{2d_{ga}}{1+\sqrt{\mu}}\right) \quad (1)$$

involving cathode to grid distance d_{kg}, grid to anode distance d_{ga}, amplification factor μ and anode voltage E_{HT}. In the above expression, the effective grid voltage has been taken to be E_{HT}/μ. But, in the case of an oscillator working under class C conditions, the effective voltage at the grid when the electron that left the cathode just when the grid started on its positive cycle reaches the grid plane is shown in the Appendix to be

$$(-E_{GB} + E_{HT}/\mu) + (E_g - E_a/\mu)\cos(\theta_a/2 - \theta_{kg})$$

where

E_{HT}, E_{GB} = steady anode and grid supply voltages

E_a, E_g = amplitudes of alternating components of anode and grid voltages

e_a, e_g = instantaneous anode and grid voltages.

Hence the cathode to grid time of flight τ_{kg} can be shown to be

$$\tau_{kg} = \frac{3d_{kg}\sqrt{(m/2e)}}{\sqrt{[(-E_{GB} + E_{HT}/\mu) + (E_g - E_a/\mu)\cos(\theta_{kg} - \theta_g/2)]}} \quad \ldots\ldots\ldots\ldots (2)$$

where m/e is the ratio of mass to the charge of an electron.

Assuming negligible space-charge effect in the grid-anode space, the transit time τ_{ga} for an electron which leaves the grid when the grid is at its positive peak is given by the following expression. It may be mentioned that the electron which left the cathode at the instant the grid

MS accepted by the Editor, January 1949

started on its positive cycle reaches the grid at the instant that the grid voltage attains its positive peak. If $E_g > E_{HT}/\mu$ (Appendix)

$$\tau_{ga} = \frac{2}{B \times 5.93 \times 10^7}\{\sqrt{(A + B \cdot d_{ga})} - \sqrt{A}\}$$

where

$$A = (E_{HT}\mu - E_{GB}) + (E_g - E_a/\mu)$$

$$B = \left[\{E_{HT} - (E_{HT}/\mu - E_{GB})\} - \{E_a + (E_g - E_a/\mu)\}\right] d_{ga}$$

The total cathode to anode time of flight τ is, therefore, given by

$$\tau = \tau_{kg} + \tau_{ga} = \frac{\sqrt{\mu}}{5.93 \times 10^7 \sqrt{E_{HT}}} \cdot \left\{3d_{kg} + \frac{2d_{ga}}{1 + \sqrt{\mu}}\right\}$$

when we neglect the alternating voltages on the electrodes and the bias on the grid. This is the same expression as that given by Gavin.[1]

The expression (2) is not readily useful for evaluating the transit time as it involves θ_{kg} and θ_g, but certain important conclusions can be drawn. When the amplitude of the alternating voltage on the grid is $1/\mu$ times the amplitude of the alternating anode voltage, then for an electron which leaves the cathode at the instant at which the grid starts becoming positive, the transit time τ_{kg} is independent of the amplitudes of the alternating voltages on the grid and anode. Another important feature is that when there is no lag (i.e., $\theta_{kg} = \theta_g/2$) the transit time τ_{kg} is reduced to a minimum if $E_g > E_{HT}/\mu$ as given by the following expression

$$\tau_{kg} = \frac{3d_{kg} \cdot \sqrt{(m/2e)}}{\sqrt{\left(-E_{GB} + \frac{E_{HT}}{\mu}\right) + \left(E_g - \frac{E_a}{\mu}\right)}} = \frac{3d_{kg} \cdot \sqrt{(m/2e)}}{\sqrt{\frac{E_{a(min)}}{\mu} + E_{g(max)}}} = \frac{3d_{kg}}{5.93 \times 10^7 \sqrt{A}}$$

Investigations by Gavin[1] show that the limiting frequency of oscillation is reached when the period of oscillation generated becomes equal to twice that of electron transit, whereas the result of Wagener[11] shows that the limiting frequency is reached when the cathode-to-grid transit time is one-sixth the period of oscillation. This difference is perhaps due to the difference in structures of the valves investigated. Modern technique has made it possible to evolve various valve structures in an attempt to extend the frequency range and useful output. So it has been thought worthwhile to study experimentally the effect of transit time on the output and efficiency and also to find the limiting frequency of oscillation of some of the available valves having different electrode structures.

Results and Discussion

Variation of power output with frequency for different valves (Fig. 1) shows the inevitable reduction in output with increasing frequency. Using dimensional analysis, Lehmann and Vallarino[12] have shown that power output W is given by the following expression.

$$W = H_4 (J^5/f^{10})$$

where H_4 is a constant, J denotes current density and f is the frequency in megacycles per second. The above expression signifies that for the same type of cathode, the power available from a valve drops very rapidly with increasing frequency. Though the above relation does not quantitatively represent the practical cases it clearly indicates that, to maintain considerable output, the current density $J = \rho v$ per unit area must be maintained at a high value, by making the charge density ρ and/or the speed of electrons v high. Two more facts are significant; first, the curves having the same general shape, it may be said that the same factors are responsible for limiting the output; secondly, that curves for some of the valves approach a limiting curve, shown by the dotted line. This common asymptote indicates that some common physical limitation is present. Moreover, greater power is available from larger valves at lower frequencies, but decay of output starts at lower frequencies for these valves.

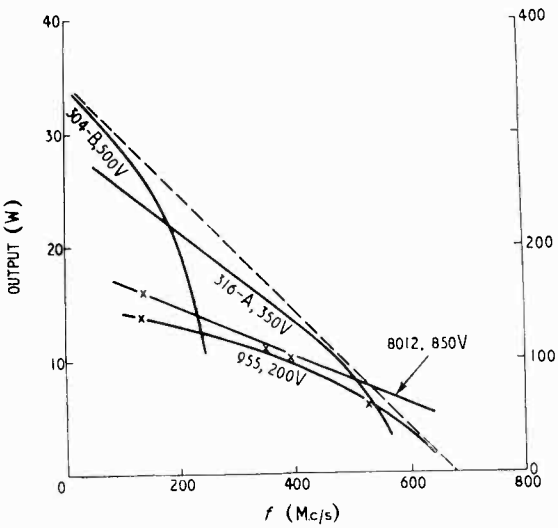

Fig. 1. *Variation of output with frequency for different types of valve. The dotted line shows that the curves approach a limiting condition.*

The inherent losses in the functioning of vacuum valves results from the degradation of kinetic energy of the electrons into heat at impact on the electrode surface. Consequently, efficiency η

depends on the motion of electrons. Efficiency being a dimensionless parameter, it has been shown[12] that $fd/\sqrt{V}$ (where d is the cathode-anode distance in cm and V is the anode potential in volts) can be represented by a dimensionless parameter, so the expression for η can be written as follows

$$\eta = u(\phi, \theta_1, \theta_2 \ldots \theta_n)$$

where ϕ is a dimensionless parameter and is taken to be equal to $fd/\sqrt{V}$ and the θ terms are dimensionless parameters, containing ϕ and describing conditions of adjustment of the oscillating circuit. If the θ terms are so chosen that η becomes a maximum η_{max} then $\eta_{max} = u(\phi)$, where one value of ϕ corresponds to a unique value of η_{max}. The variation of η with $fd/\sqrt{V}$ (Fig. 2) indicates the maximum efficiency realisable under specific conditions.

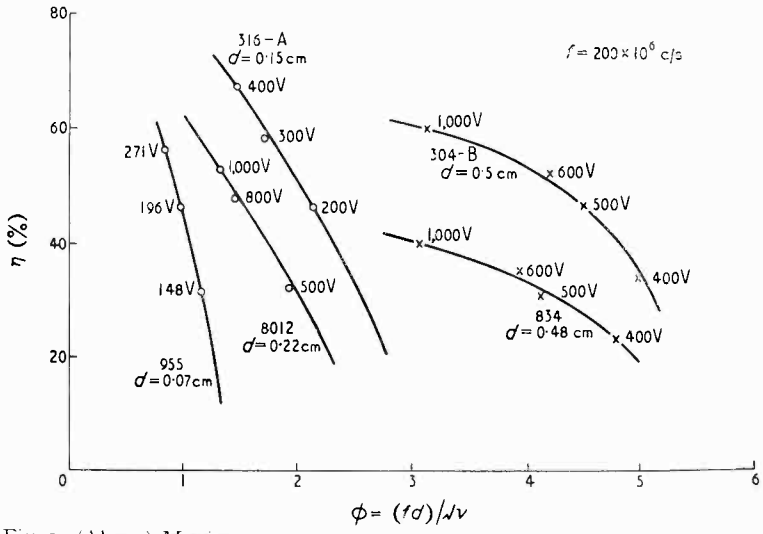

Fig. 2. (Above) *Maximum efficiency realizable under specific conditions*

Fig. 3 (right). *Efficiency versus transit angle. The limit of oscillation is found from the point where the dotted curves meet the horizontal axis.*

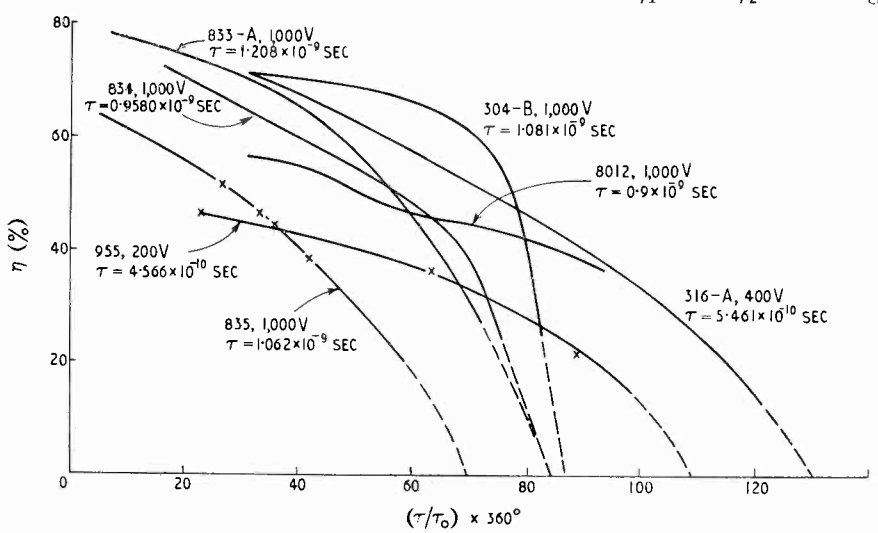

To study the effect of transit time Equ. (1) has been employed. Substituting the proper values for d_{gg} and d_{kg}, Equ. (1) can be written as follows

$$\tau_{316\text{-}A} = \frac{2.54 \times 0.255}{5.93 \times 10^7 \sqrt{E_{HT}}}$$

$$\tau_{8012} = \frac{4.243 \times 0.398}{5.93 \times 10^7 \sqrt{E_{HT}}}$$

$$\tau_{955} = \frac{5 \times 0.0766}{5.93 \times 10^7 \sqrt{E_{HT}}}$$

where the subscript to τ indicates the valve type number.

If τ_0 represents the period of oscillation, then the transit angle, $\tau/\tau_0 \times 360°$, at which a particular valve reaches its limit of oscillation is shown by extrapolating the curves of efficiency η v. transit angle (Fig. 3). The transit angle corresponding to the frequency limit of each valve is given in Table I.

It will be observed that for valves 833-A, 304-B and 834 the limiting frequency of oscillation is reached when the period of oscillation is nearly four times the time of transit of electrons from cathode to anode. In the case of 316-A and 955 the transit time corresponding to the limiting frequency is nearly one-third the period of oscillation.

The effect of transit time on efficiency can further be studied by calculating the differences in efficiencies η_1 and η_2 at a long wavelength and at a particular ultra-short wavelength. The difference in efficiencies for class C oscillators is given[1] by the following expression

$$\eta_1 - \eta_2 = \frac{\sqrt{2}}{\pi}\left(\frac{E}{E_{HT}}\right)\omega_0^2\tau^2 \quad \ldots \quad \ldots \quad (3)$$

where E/E_{HT} denotes the ratio of peak alternating voltage to the mean voltage of the anode and ω_0 represents the angular frequency corres-

ponding to the frequency of oscillation and τ represents the transit time. Taking $E/E_{HT} = 0.9$ and η_1 corresponding to the efficiency at long wavelength, the difference in efficiencies $\eta_1 - \eta_2$ can be calculated. The result is given in Fig. 4 for the 304-B valve. It will be observed that there is fair agreement between theoretical and experimental values.

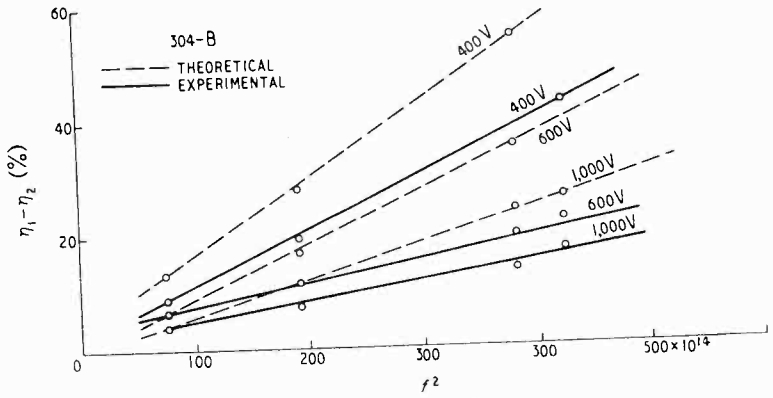

Fig. 4. *Comparison of theoretical and experimental values of the fall of efficiency with f^2.*

TABLE I

Transit angle corresponding to limiting frequency.

Valve	Anode voltage (V)	Transit angle (°)	Limiting frequency (Mc/s)
835	1,000	70	183.5
833-A	1,000	85	195.4
304-B	1,000	86	220.8
834	1,000	84	243.5
8012	1,000	>200	>600
316-A	400	130	661.2
955	200	110	669.1

TABLE II

Valve	λ_1 observed (cm)	λ_1 calculated (cm)	λ_2 observed (cm)	λ_2 calculated (cm)
835	600	530.9	171.4	174.4
833-A	600	657.7	176.5	219.2
304-B	448.9	505.9	145.9	168.7
834	397.9	467.9	129.3	152.5
8012	—	290.9	46.40	97
316-A	214.3	290.0	46.87	94.88
955	187.5	155.5	48	51.88

The wavelength λ_1 at which the efficiency drops by 10% of the maximum efficiency realizable can be calculated from Equs. (1) and (3). Similarly the wavelength λ_2 at which the efficiency is reduced to 10% of the maximum value can also be derived. For example, for valve 316-A,

$$\lambda_1 = \frac{2 \times 10^4 \times 0.29}{\sqrt{E_{HT}}} \text{ cm}$$

$$\lambda_2 = \frac{6.67 \times 10^3 \times 0.29}{\sqrt{E_{HT}}} \text{ cm}$$

The values of λ_1 and λ_2 both theoretical and experimental are given in Table II.

It will be observed that in almost all cases the calculated values of λ_1 and λ_2 are higher than the observed values. The difference, particularly in the cases of the 316-A and 8012 valves, is considerable. In the case of the 8012, the observed limiting frequency is nearly twice the calculated value. This is in agreement with the results obtained by Samuel[14] for double-ended operation.

Acknowledgment

The authors express their grateful thanks to the Head of the department for giving facilities to carry out the investigation.

APPENDIX

Transit time between cathode and grid :

e_a (Instantaneous anode voltage) $= E_{HT} - E_a \sin \omega t$

e_g (Instantaneous grid voltage) $= -E_{GB} + E_g \sin \omega t$

where E_a and E_g represent the amplitudes of the alternating components of the anode and grid voltages respectively, and E_{HT} and E_{GB} represent the steady supply voltages to anode and grid respectively.

Assume an electron leaving the cathode at time t_1 (i.e., when the grid just starts on its positive cycle) and arriving at the grid at an instant t_2. Then $\tau_{kg} = t_2 - t_1$. At t_2

$$e_a = E_{HT} - E_a \sin \omega t_2$$
$$= E_{HT} - E_a \sin \omega (T/4 - t_g/2 + t_2 - t_1)$$
$$= E_{HT} - E_a \sin \omega (T/4 - t_g/2 + \tau_{kg})$$

and $e_g = -E_{GB} + E_g \sin \omega (T/4 - t_g/2 + \tau_{kg})$

The effective voltage on the grid at instant t_2 is given by

$$\left(e_g + \frac{e_a}{\mu}\right) = \left(-E_{GB} + \frac{E_{HT}}{\mu}\right) + \left(E_g - \frac{E_a}{\mu}\right)\left\{\sin \omega \left(\frac{T}{4} - \frac{t_g}{2} + \tau_{kg}\right)\right\}$$

$$= \left(-E_{GB} + \frac{E_{HT}}{\mu}\right) + \left(E_g - \frac{E_a}{\mu}\right)\left\{\cos\left(\theta_{kg} - \frac{\theta_g}{2}\right)\right\}$$

where, $\frac{2\pi}{T} \cdot \frac{t_g}{2} = \frac{\theta_g}{2}$ = Half the angle of grid current flow,

and $\frac{2\pi}{T} \cdot \tau_{kg} = \theta_{kg}$ = Transit angle.

Hence τ_{kg} given by Gavin[1] can be modified to

$$\tau_{kg} = \frac{3d_{kg}\sqrt{(m/2e)}}{\sqrt{\left[\left(-E_{GB}+\frac{E_{HT}}{\mu}\right)+\left(E_g-\frac{E_a}{\mu}\right)\cdot\cos\left(\theta_{kg}-\frac{\theta_g}{2}\right)\right]}}$$

Transit time between grid and anode :

Let v be the velocity of an electron when it is at a distance x from the grid, at time t. Then the time of flight between grid and anode is given by the following expression :

$$\tau_{ga} = \int_0^{d_{ga}} \frac{dx}{v}$$

The potential at a point distant x from the grid at time t = potential at the grid plane at time t + potential gradient between plate and grid multiplied by x.

Therefore, the potential at x at time t is given by

$$V(x,t) = \left(e_g+\frac{e_a}{\mu}\right)+\left\{e_a-\left(e_g+\frac{e_a}{\mu}\right)\right\}\frac{x}{d_{ga}}$$

Writing,

$$e_g = -E_{GB}+E_g\cos\omega t$$
$$e_a = E_{HT}-E_a\cos\omega t$$

where t = 0 is the instant at which the electron arrives at the grid plane, which is the same as the instant at which the grid is at its positive peak, the expression for $V(x,t)$ reduces to

$$V(x,t) = \left[\left(\frac{E_{HT}}{\mu}-E_{GB}\right)+\left\{E_{HT}-\left(\frac{E_{HT}}{\mu}-E_{GB}\right)\right\}\frac{x}{d_{ga}}\right] + \left[\left(E_g-\frac{E_a}{\mu}\right)+\left\{-E_a-\left(E_g-\frac{E_a}{\mu}\right)\right\}\frac{x}{d_{ga}}\right]\cdot\cos\omega t$$

The velocity of the electron at x at time t is therefore given by

$$v(x,t) = \sqrt{\frac{2e}{m}}\cdot\sqrt{V(x,t)} = 5.93\times10^7\sqrt{V(x,t)}$$

At time t = 0, $\cos\omega t$ = 1. In most cases τ_{ga} is of the order of 10^{-9} to 10^{-10} second. Therefore, in practical cases, as $\omega t = 2\pi\cdot t/T$, $\cos\omega t$ may be taken as unity up to 100 Mc/s. The expression for $V(x,t)$ then reduces to

$$V(x,t) = \left[\left(\frac{E_{HT}}{\mu}-E_{GB}\right)+\left(E_g-\frac{E_a}{\mu}\right)\right]+ x\left[\frac{1}{d_{ga}}\left\{E_{HT}-\left(\frac{E_{HT}}{\mu}-E_{GB}\right)\right\}-\frac{1}{d_{ga}}\left\{E_a+\left(E_g-\frac{E_a}{\mu}\right)\right\}\right]$$
$$= A+Bx$$

$$\therefore \tau_{ga} = \int_0^{d_{ga}}\frac{dx}{5.93\times10^7\sqrt{(A+Bx)}} = \frac{2}{5.93\times10^7}\cdot\left\{\frac{\sqrt{(A+Bd_{ga})}-\sqrt{A}}{B}\right\}$$

REFERENCES

1. M. R Gavin, *Wireless Engineer*, 1939, Vol. 16, p. 287.
2. A. Scheibe, *Ann. der. Physik*, 1924, Vol. 82, p. 54.
3. F. B. Llewellyn, *Proc. Inst. Radio Engrs*, 1935, Vol. 23, p. 112.
4. D. O. North, *Proc. Inst. Radio Engrs*, 1936, Vol. 24, p. 108.
5. W. E. Benham, *Phil Mag. Supp.*, 1931, Vol. 11, p. 457.
6. J. S. McPetrie, *Phil Mag.*, 1933, Vol. 16, p. 284, 544.
7. F. B. Llewellyn, *Proc. Inst. Radio Engrs*, 1933, Vol. 25, p. 1532; *Bell Syst tech. J.*, 1935, Vol. 14, p. 632.
8. Chao-Chan-Wang, *Proc. Inst. Radio Engrs*, 1941, Vol. 29, p. 200.
9. C. L. Fortescue, *Wireless Engineer*, 1935, Vol. 12, p. 310.
10. R. Kompfner, *Wireless Engineer*, 1942, Vol. 19, p. 2.
11. W. G. Wagener, *Proc. Inst. Radio Engrs*, 1938, Vol. 26, p. 401.
12. G. J. Lehmann and A. R. Vallarino, *Proc. Inst. Radio Engrs*, 1945, Vol. 33, p. 663.
13. L. Langmuir, *Physical Review*, 1913, Vol. 2, p. 450.
14. A. L. Samuel, *J. appl. Phys.*, 1937, Vol. 8, p. 677.

CORRESPONDENCE

Letters to the Editor on technical subjects are always welcome. In publishing such communications the Editors do not necessarily endorse any technical or general statements which they may contain.

Secondary-Emission Tubes in Wideband Amplifiers

SIR,—With reference to the letter by N. F. Moody and G. J. R. McLusky on the above subject, published in your December issue, it may be of interest to note that the described method of obtaining push-pull output from anode and dynode of a secondary-emission valve was invented by E. V. Truefitt as early as 1937 when the TSE4 first became available. This invention is described in the specification of British Patent No. 508,038 which was published in 1939.

C. FALCONER CHAPTER

Cinema-Television, Ltd.,
London.

The Intrinsic Impedance of Space

SIR,—The fact that the technical literature mentions this impedance as being sometimes 377 ohms and at other times 30 ohms is misleading. I shall attempt to clear away this confusion.

The systems of units may differ both through the choice of the fundamental quantities and through the choice of the defining equations of the derived units so as to determine in a certain manner the value of the parasitic coefficients.

For instance, the area of a square which may be expressed in general through the formula, $s = al$, becomes specifically :

in the metric system :

$s = l^2$ square meters, where l is measured in meters,

in the Anglo-American system :

$s = l^2$ square inches, where l is measured in inches,

in the American circular system :

$s = \frac{4l^2}{\pi}$ circular inches, where l is measured in inches.

In the first two formulae the factor taken as equal to 1 is the parasitic coefficient of the formula giving the area of the square, whereas in the latter system the factor taken as equal to 1 is the coefficient of the formula giving the area of the circle.

The first choice is equivalent to taking the square of 1-m or 1-in side as the unit for areas, while the second one is equivalent to adopting the circle of 1-in diameter as the unit for areas.

Consequently, when the system of measuring units is changed, it must be expected, in general, that a number of units will have their magnitudes altered and some forms of the equations defining the corresponding quantities will be equally altered.

It is true that usually the systems are based on the

same forms of the defining equations, so that it is only a matter of changing the units when passing from one system to the other.

When, however, the problem of 'rationalizing' is raised in electricity and magnetism, the rationalized system introduced is different from the classical, non-rationalized system, not only as regards the units, but also in the forms of the defining equations.

The rationalizing may be effected in several ways, according to the formulae chosen, from which it is intended to derive the 4π factor.

In electricity and magnetism, it is noted sometimes that two quantities of different nature have the same dimension in a certain system of measuring units. For instance, in the systems using as fundamental quantities the length, the mass, the time and the intensity of the electric current, we encounter the following pairs of quantities having the same dimension :

(a) ϕ_D and q $[TI]$

(b) ϕ_B and m $[L^2MT^{-2}I^{-1}]$

(c) $Z_0 = \frac{\mathcal{E}}{H}$ and R $[L^2MT^{-3}I^{-3}]$

(d) J (intensity of magnetization) and B $[MT^{-2}I^{-1}]$

It would seem natural that these quantities should have units of the same magnitude in a particular system of units. But because of the parasitic coefficients of their defining formulae this is not the case. In some systems of units the two quantities of the same dimensions have identical units, whereas in other systems of units they have units of different magnitudes.

In the rationalized system we shall write :

$$\phi_D' = q$$

while in the non-rationalized system we write :

$$\phi_D = 4\pi q$$

While in the first system the unit of induction flow is the coulomb, in the second one it is the sterradian coulomb ; therefore, one coulomb $= 4\pi$ sterradian coulombs.

When we switch from the first system to the second one, the unit of quantity of electricity remains unchanged, while the unit of flow is changed, although these quantities always have the same dimension.

Therefore, the same flow will be expressed one time by ϕ_D and another time by ϕ_D', although the electric charge is all the time measured by q.

The same thing may be said of the units for ϕ_B and for m ; the unit of magnetic flow in the m.k.s. system is the Weber in any of its two variants, whether rationalized or not. On the other hand, the magnetic mass defined by the relation :

$$\Sigma m' = \phi_B' \text{ in the rationalized system}$$

and $4\pi\Sigma m = \phi_B$ in the non-rationalized system, will be expressed in webers in the rationalized system and in other units (newtons by millioersteds) in the non-rationalized system. This explains the different values assumed by Z_0, the intrinsic impedance of space, according to the system, rationalized or non-rationalized, in which it is expressed.

Z_0 is of the nature of an impedance and is defined by the equation :

$$Z_0 = \mathcal{E}/H$$

Since $\mathcal{E}$ remains unchanged when switching from the non-rationalized varient to the rationalized one, while H changes (in the non-rationalized system we have $\int H dl = 4\pi\Sigma I$ whereas in the rationalized system $\int H' dl = \Sigma I$), it follows that Z_0 will have different units and consequently different values in each of the two variants.

In his Editorial of September 1949, Prof. G. W. O. Howe, reasoning on the case of a line 'consisting of two parallel flat strips,' shows that the intrinsic impedance $\mathcal{E}/H$ written in the rationalized system is expressed by :

$$Z = V/I$$

which is measured in ohms. On the basis of this practical observation we may draw the conclusion that Z_0 will be expressed in ohms only in the rationalized system (377 ohms), while in the non-rationalized system, where Z_0 has 30 as its numerical value, the units will be different (volts by millioersted and meter) :

$$\frac{\text{volts}}{\text{millioersted} \times \text{metre}} = 4\pi \text{ ohms.}$$

Thus, the intrinsic impedance of 30 volts by millioersted and meter, converted to ohms gives the same value of 377 ohms. Consequently, it may not be spoken of anything else than 377 ohms, *it being an error to say that the intrinsic impedance of space is* 30 *ohms.* If we change the definition of Z_0, stating that $Z_0 = \frac{\mathcal{E}}{H}$ in the rationalized system and $Z_0 = 4\pi\frac{\mathcal{E}}{H}$ in the non-rationalized system then the result in non-rationalized units is expressed equally in ohms, but its value is 377 and not 30 ohms.

T. TANASESCU

The Polytechnic Institute of Bucharest.

MONSIEUR,—Dans son numero de septembre dernier, votre Revue a publié sous le titre " The intrinsic impedance of space " et sous les initiales G.W.O.H., une critique de ma note du 18 février dernier à l'Académie des Sciences de Paris, dans laquelle le nom de M. Louis de Broglie a été accolé au mien, alors que, suivant l'usage français, son intervention s'est bornée à soumettre cette note au jugement de l'Académie. Monsieur de Broglie ne saurait donc encourir aucune responsabilité du fait de son contenu.

Je suis certain que vous voudrez bien faire connaître à vos lecteurs dans le plus bref délai, que le savant éminent qu'est Monsieur de Broglie ne devait pas être mis en cause dans cette discussion.

Je vous signale que l'erreur typographique concernant la valeur 477 ohms au lieu de 377 ohms a été signalée dans le numero de mai 1949 de la *Revue générale de l'Electricité*, page 168, note 1.

Asnieres, Paris. E. BRYLINSKI

Detuned Resonant Circuits.

SIR,—The article under this title, by H. Elger, in the November 1949 issue of *Wireless Engineer* (p. 360), seems to contain a rather serious error in the determination of transient response. The author states that at high frequencies the phase of the exciting voltage at $t = 0$ can be assumed equal to zero ; this is remarkable, as surely the effect of the initial phase is the same in whatever frequency band the circuit is used. The initial phase has a negligible effect when the applied signal has the same frequency as resonance (i.e., $\omega = \omega_0$) so that equation (2c) is correct, but for all other frequencies of applied signal the effect is appreciable, so that equations (2a) and (2b) do not give an adequate statement of the response. This matter is brought out clearly in standard texts such as Guillemin[1] and in an article by myself.[2] If the suddenly-applied signal is proportional to $\sin(\omega t + \psi)$, and E is the steady-state peak output, then when ω is considerably different from ω_0, the tran-

[1] Guillemin, E. A., "Communication Networks," Vol. 1, p. 95 onwards (John Wiley, 1931).

[2] Tucker, D. G., "The Transient Response of a Tuned Circuit," *Electronic Engng*, 1946, Vol. 18, p. 379–381.

sient output e is given for the two extreme cases of initial phase, thus—

$$\left.\begin{aligned} \psi = 0,\ \frac{e}{E} &\approx \cos \omega t - e^{-\omega_0 t/2Q} \cos \omega_0 t \\ \psi = \frac{\pi}{2},\ \frac{e}{E} &\approx \sin \omega t - \frac{\omega_0}{\omega} e^{-\omega_0 t/2Q} \sin \omega_0 t \end{aligned}\right\}$$

which should replace Mr. Elger's equation (2a), and the switching-off transients are

$$\left.\begin{aligned} \psi = 0,\ \frac{e}{E} &= e^{-\omega_0 t/2Q} \cos \omega_0 t \\ \psi = \frac{\pi}{2},\ \frac{e}{E} &= \frac{\omega_0}{\omega} e^{-\omega_0 t/2Q} \sin \omega_0 t \end{aligned}\right\}$$

replacing equation (2b).

It can be seen that the purely transient component of the output can be affected in the ratio $\frac{\omega_0}{\omega}$ according to initial phase. For small detuning this may be an inappreciable effect, but Mr. Elger is certainly not justified in ignoring it when the detuning is 'excessive' (see last paragraph on p. 362). In actual fact, peak amplitudes when $\omega \ll \omega_0$ may run to ten or a hundred times the steady-state amplitude, and not just to twice, as Mr. Elger states. This is illustrated by oscillograms in my article. Moreover, in practice it is necessary to consider the response to signals outside the normal acceptance band, because although their steady-state effect may be negligible, the transient they produce may cause serious interference.

Post Office Research Station. D. G. TUCKER

SIR,—The mathematical statement of Mr. D. G. Tucker is quite correct and can easily be derived from my equation (1). In the publication[3] of Fraenckel it is shown by numerical examples that the peak voltage (or current) may materially exceed the value $2E$. My statement that the phase ψ may be assumed to be equal to zero at high frequencies is, of course, not dependent on the frequency itself but on the practical use made of the different frequency ranges. It is evidently not necessary to explain the differences involved in problems relating to, say, power transmission at mains frequency and radar technique.

Mr. Tucker seems to have overlooked my statements preceding the equations (2a) and (3a) where I have expressly stated the conditions $\Delta\omega \ll \omega_0$ and $Q \gg 1$. At high frequency, 'excessive detuning' means any detuning beyond the bandwidth limits $Qv = 0.5$; i.e., a detuning exceeding 5% at $Q = 10$. In order to enable the reader to deal with other similar problems outside my theory I have indicated the equation (1).

My theory covers transients at least at $Qv = 4$ (see Fig. 4 and the well-known range of the normal universal resonance curve) $Q \geqslant 10$ and $\Delta\omega \ll \omega_0$. Equation (3a) in its present form yields $e_{max} = 2E$ and, if developed with $\psi = 90°$, $e_{max} = 1 + \omega_0/\omega$. If we now take the above extreme values applied to *any* frequency, we thus obtain $v_{max} = 25\%$ and the absolute maximum values $e = 2E$ and $e = 2.33E$ respectively and thus my 'serious error' can amount at most to nearly 17%; this means the extreme ends of my curve b in Fig. 4 may rise by 1.5 mm. Actually, the error will be much less since I have assumed the extreme and impossible case that the first peak occurs at $t = 0$ and thus coincides with the e/E axis of Fig. 3.

As to the last sentence of Mr. Tucker, he agrees with me that the response to signals (interference) outside the normal acceptance band should be considered and I had, therefore, shown the response within a range 8 times wider than the normal bandwidth. In practice it is evidently not necessary to calculate the response to interference far off the bandwith with any greater degree of accuracy if it is ever considered necessary to make numerical calculations at all. It is much more important to show that a clear and qualitative result is universally applicable (at the higher frequencies) and to give a distinct general conception of the transients in such cases.

I am, however, indebted to Mr. Tucker for drawing my attention to his publication and that of Guillemin which I had not seen until now due to particularly unfavourable circumstances at the time in question.

Stockholm, Sweden. H. ELGER

A Problem

A reader asks if anyone can suggest, or give a reference to a published description of, a method of finding the conditions under which

$$\int_{c-j\infty}^{c+j\infty} f(\lambda) e^{\lambda t}\, d\lambda$$

is monotonic in t and yet has the fastest rate of rise.—[ED.]

Phase-Shift Oscillator

SIR,—I was very interested to see W. C. Vaughan's analysis in the December *Wireless Engineer* which, although extremely ingenious, fails to take into account the internal impedance of the driving source.

The effect of this internal impedance can seldom be neglected, and after all, one of the chief advantages of the phase-shift oscillator is the precision with which it can be designed and made. Your readers may, therefore, be interested in an article of mine in the January 1950 issue of *Electronic Engineering* which demonstrates a comprehensive and flexible method of analysis by simple matrix algebra, and gives design formulæ which are free from approximations.

The matrix method is comprehensive because it provides the voltage ratio and input impedance of a four-terminal network simultaneously, and requires no special conditions concerning the similarity of transmission sections as it includes all valves and coupling arrangements.

The other advantage of flexibility enables a critical analysis to be made of an existing design, as it is comparatively easy to calculate the effect of changes in network elements.

Staines, Middlesex. W. R. HINTON

SIR,—Referring to W. C. Vaughan's article in the December 1949 *Wireless Engineer*, I feel that one general conclusion which might have been drawn from Tables I and II is that the networks containing shunt reactances may be used more profitably at high frequencies than those containing shunt resistances, while these latter are preferable at low frequencies. This is clear from the expressions for frequency since a greater CR product may be used in the former case than in the latter for a given frequency. This applies particularly to 3-mesh networks.

It is also suggested that the anode-load should be much less than the network input impedance—which might usefully have been tabulated—though no mention is made of a possibility of avoiding phase-shift in the valve altogether. In every case where shunt reactances are used the first resistance may be formed from the anode load in parallel with the valve's internal resistance. The first capacitance may then be formed, at least partly, by the anode–cathode capacitance and the last by the capacitance between grid and cathode. This is very useful

at high frequencies; e.g., for a 3-mesh network, if $R = 10^4$ MΩ, $C = 10$ pF and $n = 1$, $f = 3.9$ Mc/s.

Finally it is not obvious to me why the output waveform should be inherently better than with conventional LC circuits. This may be true at very low frequencies, but is surely not generally true.

Gt. Malvern, Worcs. W. P. N. COURT

Non-linear Effects in Rectifier Modulators.

SIR,—V. Belevitch gave a most interesting analysis of the nonlinear operation of a ring modulator in *Wireless Engineer*, May 1949, Vol. 26, p. 177, and stated also that the results applied equally to the bridge (otherwise known as shunt or Cowan) modulator with suitable adjustment, such as 6 db in the level of the products, etc. This analysis was based on a sinusoidal carrier and on the conception of the ideal rectifier; i.e., one with zero forward resistance and infinite backward resistance, changing over at zero voltage across it. Now this basis is very useful for analysing the performance of modulators in the linear condition, where the signal has no influence on the switching of the rectifier. However, we very much question its utility in the non-linear case, and would like to suggest that analytical results approaching those obtained in practice can be expected only by a more realistic approach.

No real rectifier switches from low to high resistance at the instant when the carrier (or bias) voltage changes polarity. There is always a transition interval, where non-linearity occurs not so much because the signal may exceed the carrier voltage and thus determine the time of 'switching' (as in Dr. Belevitch's ideal case), but rather because the rectifier resistance varies steeply

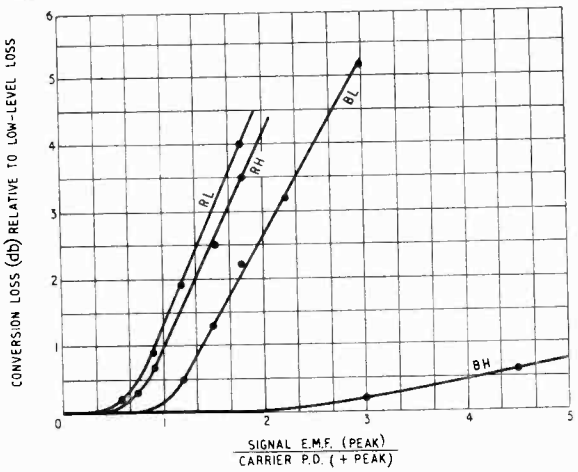

Fig. 1. *Overload characteristics of ring and bridge modulators.*

with voltage, and intermodulation and overloading occur. It is thus better to consider as an 'ideal' case for analysis one in which a square-wave carrier is used, so that in the absence of the signal the rectifiers switch from forward to backward resistance instantly. Whether the rectifiers are ideal or not has now less bearing on the result, which can consequently accord better with measurements. The mathematical analysis is no more complicated than in the sinusoidal case.

This conception of square-wave switching is approximated fairly closely by a practical case where a sinusoidal carrier e.m.f. is applied through a high resistance. We shall find that in such a case we obtain results very different from those given by Dr. Belevitch.

It is also inconvenient to consider rectifiers with zero forward resistance, since the carrier voltage can be developed across them only if the carrier source resistance (hereafter referred to as c.s.r.) is zero. Since, as we shall see, the question of c.s.r. is vital in the consideration of the bridge modulator, we should restrict our analysis to finite forward resistance.

In the ring modulator overload occurs when the signal voltage equals the carrier voltage across one of the rectifiers which is nominally in the blocking condition.

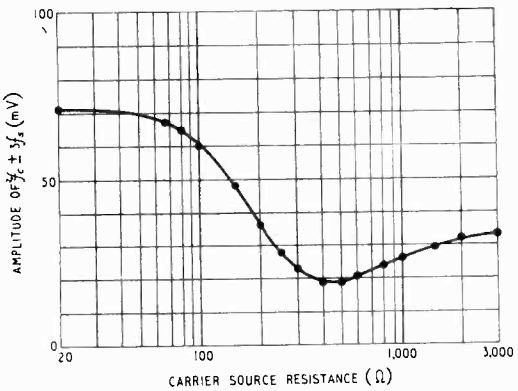

Fig. 2. *Harmonic distortion in bridge modulator.*

This does actually give an overload point corresponding very roughly to that shown by Dr. Belevitch. But in the conventional bridge modulator failure of the blocking condition in this way causes overload only in so far as the c.s.r., which is then thrown across the signal circuit, is low enough to prevent efficient modulation. Thus with a high c.s.r. overload cannot occur due to such a cause, and will only occur when the signal and carrier voltages across the forward resistance of each rectifier become equal—then one rectifier of each series pair becomes blocking and modulation fails. This occurs only at very high signal e.m.fs. The c.s.r. now limits the resistance to which the blocking due to overload can rise, and consequently a very high c.s.r. gives a more rapid overload than one less high. We thus find that there is an optimum c.s.r. which gives the highest overload point (and, in practice, the smallest nonlinear distortion below overload), and this has a value of the order of the circuit resistance (i.e., signal source and load in parallel).

Fig. 1 shows measured overload characteristics of ring (R) and bridge (B) modulators with low (L) and high (H) carrier source resistances. The terms 'low' and 'high' are relative to the forward resistance of the rectifiers which were copper-oxide type KG1; the carrier p.d. was 0.5 V peak for the ring and 1.0 V positive peak for the bridge (i.e., 0.5 V per rectifier in both cases), and the frequencies were 11 kc/s for the carrier and 500 c/s for the signal. The circuit resistance was 3,000 ohms, and the high c.s.r. was 1,000 ohms.

Fig. 2 shows measured harmonic distortion of the type $f_c \pm 3f_s$, in a bridge modulator, as a function of c.s.r. Here germanium rectifiers (CG1C) were used, with 2-V carrier (positive peak), 6-V signal e.m.f. and $R = 500$ ohms. It can be seen that the experimental results confirm the theoretical discussion.

A further point regarding bridge modulators is that the carrier voltage is greater across the backward than across the forward resistance unless steps are taken to equalize it by means of another rectifier or another modulator, connected in opposite polarity, in parallel with the carrier; this then becomes part of the c.s.r.

Post Office Research Station. D. G. TUCKER, E. JEYNES

NEW BOOKS

Radio Aerials

By E. B. MOULLIN, M.A., Sc.D. Pp. 514 + xi. Oxford University Press, Amen House, Warwick Sq., London, E.C.4. Price 50s.

This is one of a series of monographs intended to provide accounts of recent advances in the scientific field. It deals only with a limited class of radio aerials, but does so in great detail.

The book is divided into two sections, one theoretical and the other experimental. In the former, after establishing Maxwell's equations and the Lorentz retarded potential functions the formulæ are used to calculate the fields due to current filaments, the effect of flat sheet and V reflectors and problems relating to cylinders immersed in electromagnetic fields. Arrays of radiating elements are then considered, the power gain calculated, and methods of suppressing the side lobes discussed. A short section is devoted to the isolated aerial, where attempts at a rigorous solution are mentioned, but not discussed in detail.

The remainder of the book is devoted to experimental procedure and measurements of aerial performance, mainly those made on the type of aerial described in the first section. Results for V reflectors are given in great detail, and many practical design considerations discussed.

The treatment is mainly mathematical; many of the problems concerned are hypothetical, and are included to illustrate the analytical methods. The solutions are later used to good effect, however, in obtaining approximate solutions of cases which cannot be solved rigorously, or where the rigorous solution would be too complicated to help in the understanding of the problem.

Throughout the book the author gives physical interpretations of the methods and results, which will appeal to the reader who likes to understand the significance of the mathematics as he goes along. This useful feature contributes greatly to the value and interest of the book.

In the calculation of radiation resistance, the author often refers to the value of the field at the surface of wires; inasmuch as no field tangential to the surface of a perfectly conducting wire can exist this statement needs qualification. If the postulated current distribution results in a tangential component of field, it means that it can only be sustained by using a series of generators distributed along the wire; the power supplied by these generators is then equal to the radiated power and is calculated by the method used by the author. If only one generator is supplied, the current distribution will adjust itself until the tangential component of field is zero along the wire.

This is, however, a minor criticism of a valuable addition to the literature on radio aerials. It is recommended, not only as a reference book on the types of aerial described, but also for the clear and logical development of the general theory.

H. P.

List of Preferred Valves

Pp. 28. The Scientific Instrument Manufacturers' Association of Great Britain Ltd., 17, Princes Gate, London, S.W.7. Price 2s. 6d.

This list of valves comprises types which are recommended by the Association for use in electronic instruments in order to limit the number of types used. The valves are chiefly ones with the IO and B7G bases. Abbreviated characteristics and base connections are included.

A Symposium on Electronics in Research a Industry

Edited by A. G. PEACOCK. Pp. 199+xiii. Chapman & Hall Ltd., 37, Essex, St., London, W.C.2. Price 16s.

This book, which is published in collaboration with the Instrument Manufacturers' Association of Great Britain Ltd., comprises papers read at the first Electronics Symposium. The papers cover Electronics in Computing, Frequency Measurement, The Measurement of Small Displacements by Electrical and Electronic Methods, Measurement of Ionizing Radiations, High Vacuum Gauges, The Radiosonde and its Manufacture, Some Industrial Applications of Ultrasonics, Metal Detection in Industry, Sound and Vibration Measurement, Electronics in Spectroscopy, and Some Developments in Picture Telegraphy.

Electrical Transmission of Power and Signals

By EDWARD W. KINIBARK. Pp. 461. John Wiley & Sons, Inc., New York, and Chapman & Hall Ltd., 37, Essex St., London, W.C.2. Price 48s.

This book, which is of American origin, covers r.f. transmission lines and waveguides, as well as power-frequency transmission.

Photoelectricity and its Application

By V. K. ZWORYKIN, E.E., Ph.D., and E. G. RAMBERG, Ph.D. Pp. 494 + xii. John Wiley & Sons, Inc., New York, and Chapman & Hall Ltd., 37, Essex St., London, W.C.2. Price 45s.

Theory and Desig n of Electron Beams

By J. R. PIERCE. Pp. 197 + xiii. D. Van Nostrand Co. Inc., 250, Fourth Avenue, New York, U.S.A. Price $3.50.

Lateral Deviation of Radio Waves Reflected in the Ionosphere

By W. Ross, M.A., A.M.I.E.E. Radio Research Special Report No. 19. Pp. 32 + iv. H.M. Stationery Office, York House, Kingsway, London, W.C.2. Price 9d. (U.S.A. 25 cents).

This report gives the results of investigations during the years 1938-1947 into the deviations from the great-circle plane of waves reflected from the ionosphere.

Television Explained (3rd Edition)

By W. E. MILLER, M.A.(Cantab), M.Brit.I.R.E. Pp. 112 with 59 diagrams and 17 photographs. The Trader Publishing Co. Ltd., Dorset House, Stamford St., London, S.E.1. Price 5s.

Communication Circuits (3rd Edition)

By LAWRENCE A. WARE, E.E., Ph.D., and HENRY R. REED, M.S., E.E., Ph.D. Pp. 403 + x. John Wiley & Sons, Inc., New York, and Chapman & Hall Ltd., 37, Essex St., London, W.C.2. Price 40s.

F.B.I. REGISTER

The 1949/50 F.B.I. Register has over 1,000 pages and includes nearly 6,000 firms under 5,000 cross-reference headings. The sections include addresses, brands and trademarks, products and services. There are reference facilities in French and Spanish.

Published jointly by Kelly's Directories Ltd., and Iliffe & Sons Ltd. Home orders should be addressed to Kelly's Directories Ltd., 196, Strand, London, W.C.2, and overseas orders to Iliffe & Sons Ltd., Dorset House, Stamford St., London, S.E.1. The price is 42s.

WIRELESS PATENTS

A Summary of Recently Accepted Specifications

The following abstracts are prepared, with the permission of the Controller of H.M. Stationery Office, from Specifications obtainable at the Patent Office, 25, Southampton Buildings, London, W.C.2, price 2 - each.

AERIALS AND AERIAL SYSTEMS

625 413.—Aerial for aircraft wherein an insulated section of the aircraft skin has a metal film sprayed directly thereon.

Joshua Marney. Application date July 10th, 1947.

626 210.—A broadcast transmitting aerial employing a vertical radiator surrounded at its lower end by a concentric cage of subsidiary radiators, the latter having a radius of between $\lambda/100$ and $\lambda/60$.

Marconi's Wireless Telegraph Company Ltd., and H. Cafferata. Application date April 15th, 1946.

626 311.—An aerial system having a primary radiator and a reflector having a concave outer portion of parabolic form, designed so that the reflector has a ring locus.

Western Electric Company Inc. Convention date (U.S.A.) July 21st, 1945.

DIRECTIONAL AND NAVIGATIONAL SYSTEMS

626 236.—A pulse-radar system wherein the receiver embodies means for producing an oscillation at p.r. frequency (or related integrally thereto) which is combined with the received signals, the system being responsive only when the received pulse coincides in a particular manner with the local oscillation.

Marconi's Wireless Telegraph Company Ltd. (assignees of Thomas Treadwell Eaton). Convention date (U.S.A.) September 13th, 1941.

626 325.—A receiver and indicator for a beacon radiating a beam varying in frequency according to azimuth direction, and having two selective means differently variable in attenuation with frequency, the outputs from the two means being compared.

Standard Telephones and Cables Ltd. (assignees of A. Frum). Convention date (U.S.A.) June 11th, 1945.

626 610.—F. M. radio altimeter in which a voltage dependent on the speed of the modulator capacitor drive motor provides a compensating function to render this system independent of modulation frequency.

Bernard Anselm Sharpe. Application date May 3rd, 1945.

626 709.—V.H.F. high pulse-power generators using several waveguides of different propagation times and feeding into a common waveguide.

Compagnie General De Telegraphie Sans Fil. Convention date (France) March 4th, 1944.

626 870.—Receiving apparatus for beacons wherein the phase of signals from spaced transmitters is compared, consisting in using aerials having different patterns which are employed successively to avoid erroneous phase indications.

William Joseph O'Brien. Convention date (U.S.A.) August 27th, 1945.

626 956.—A radio beacon for aircraft distance indication emitting primary signals in successive directions and having distinguishing characteristics, the aircraft emitting signals having a different characteristic, the beacon retransmitting response signals to the aircraft.

Standard Telephones and Cables Limited (assignees of H. G. Busignies). Convention date (U.S.A.) August 11th, 1945.

RECEIVING CIRCUITS AND APPARATUS

(See also under Television)

626 088.—Automatic gain or frequency control in which the valve to which the control voltage is applied includes a phase-shift network to introduce a virtual capacitance into the smoothing circuit to vary the time constant thereof.

Philips Lamps Limited. Convention date (Netherlands) June 1st, 1943.

626 142.—Thermionic valve apparatus embodying independent screening chassis each of which carries a part of a valveholder, the other part of which is carried by another chassis.

Philips Lamps Ltd. Convention date (Netherlands) September 14th, 1943.

626 154.—Phase or frequency-modulated signal receiver operating on the super-regenerative principle and designed primarily to secure low distortion.

Hazeltine Corporation (assignees of B. D. Loughlin). Convention date (U.S.A.) March 19th, 1946.

626 221.—Signal-seeking receiver having motor tuning which stops on tuning to a usable signal, wherein control of the motor is made insensitive to noise by a narrow-band selector.

Colonial Radio Corporation. Convention date (U.S.A.) September 16th, 1944.

626 420.—Phase or frequency-modulation detector especially for converting such pulses to amplitude-modulated pulses, using two rectifiers and a cathode-follower stage.

Bendix Aviation Corporation. Convention date (U.S.A.) August 23rd, 1946.

626 739.—Frequency discriminator in which tuned circuits feed opposed rectifiers and also two further opposite rectifiers, the two sets of rectifiers feeding a metering circuit to indicate or monitor the modulation.

Marconi's Wireless Telegraph Company Ltd. and I. S. Forbes. Application date February 6th, 1947.

TELEVISION CIRCUITS AND APPARATUS

FOR TRANSMISSION AND RECEPTION

626 715.—Apparatus for television film transmission using two film projectors for alternative use and adjustable means for transmitting from either projector to the television camera.

H. G. De France. Convention dates (France) October 11th, 1941, August 12th, 1942.

SUBSIDIARY APPARATUS AND MATERIALS

626 129.—Permeability-tuned circuits in which coils and cores are mounted for relative movement and coupled by an auxiliary coil arranged so that the coupling coefficient varies inversely with frequency.

Marconi's Wireless Telegraph Co. Ltd. (assignees H. Ruben). Convention date (U.S.A.) May 12th, 1945.

626 620.—The dielectric of a capacitor for medium frequencies consists of an aliphatic ester of boric acid having prescribed characteristics.

The British Thomson-Houston Co. Ltd. Convention date (U.S.A.) September 1st, 1944.